Flow-Induced Vibration of a Non-Constant Tension Cable in a Sheared Flow

Peter Capozucca

B.S., University of New Hampshire (1986)

Submitted in Partial Fulfillment of the Requirements

for the Degree of Master of Science in Ocean Engineering

at the

Massachusetts Institute of Technology

September 1988

© Massachusetts Institute of Technology, 1988

Signature of Author _____

Department of Ocean Engineering
September, 1988

Certified by _____

rofessor J. Kim Vandiver
Thesis Supervisor

Accepted by _____

Professor A. Douglas Carmichael
Chairman, Department Graduate Committee

MASSACHUSETTS INSTITUTE OF TECHNOLOGY

SEP 23 1988

Archives

LIBRARIES

Abstract

In most practical marine applications, offshore structures are located in areas of strong currents and are subject to vortex induced vibration. In most situations, the tension on a long flexible cylinder is not constant along its length due to external forces acting on the structure. The purpose of this thesis is to establish an accurate response prediction model for a non-constant tension cable in a spatially varying flow.

The governing equations for the spatially varying tension cable are presented and used to solve for the systems natural frequencies and mode shapes. Given these relations, the modal damping ratios for the mainly excited modes are found. With these damping values a response prediction model based on a Greens function approach is presented.

The response model is tested for small values of tension variation and approaches the results of the corresponding constant tension case. The spatially varying tension Greens function is examined under various conditions. The function is seen to be significantly dependent on damping and to a lesser extent on tension variation. Quantitative examples showing how changes in these parameters effect Greens function response are included. Finally, results of a practical application for a 2000 foot long production riser are presented.

Contents

List of Figures

Chapter 1

Introduction

Many offshore structures are located in areas of strong currents and are subjected to vortex-induced vibration. The dynamic response of the structure must be investigated to ensure first that resonant phenomena will not cause excessive stresses and ultimately failure, and second that the dynamic response does not compromise the performance of the system.

Many previous cases involving vortex-induced vibration phenomena have been examined, including vibration of constant tension cables in uniform flows, and most recently the flow-induced vibration of a constant tension cable in a sheared flow. Ocean currents are seldom spatially or directionally uniform and can excite different cable modes at spatially varying frequencies. The doctoral thesis of T.Y. Chung [1] addressed the problem of developing a more accurate response prediction model which took into account the effect of a spatially varying flow.

The subject of this paper is to expand on that prediction model and account for cases in which the tension on the cable varies spatially. In most practical cases the tension on a flexible cylinder is not constant along its length due to drag forces and the cables own weight.

In chapter two some basic background in flow-induced vibration is given. In chapter three the governing equations for the non-constant tension cable are presented, and from these equations the characteristic mode shapes and frequencies are found. In chapter four the hydrodynamic damping model is presented, and the equivalent

damping constants and modal damping ratios are determined. In chapter five a response prediction model making use of the Greens function for the cable is used to arrive at the frequency response spectrum.

Chapter 2

Background

2.1 Flow Around Circular Cylinders

When a fluid flows around a stationary circular cylinder the flow separates and vortices are shed in the wake. As a result of this vortex shedding a periodic wake is formed causing an unsteady pressure distribution which causes the cable to oscillate in the out of plane direction with respect to the fluid flow. The ultimate configuration of vortices downstream in the wake is asymmetrical [Von Karman fig(2.1)]. The vortices are shed into the wake at the vortex shedding frequency f_s, which is a function of flow velocity V, cylinder diameter D, and Reynolds number, $R_e = \rho V D/\mu$. Then, $f_s = S_t \frac{V}{D}$, where S_t is the Strouhal number which depends on Reynolds number as shown in figure (2.2).

Due to the uneven pressure distribution on the cable a periodic lift force acts on the body. Through dimensional analysis this force can be found to depend on a local lift coefficient C_L and the group $\rho_w V^2 D$. The lift force can then be written as ,

$$F_L(x,t) = \frac{1}{2}\rho_w V^2 D C_L(x,t) \tag{2.1}$$

The lift force is not purely sinusoidal, but periodic. The exact solution includes higher harmonics of different amplitudes.

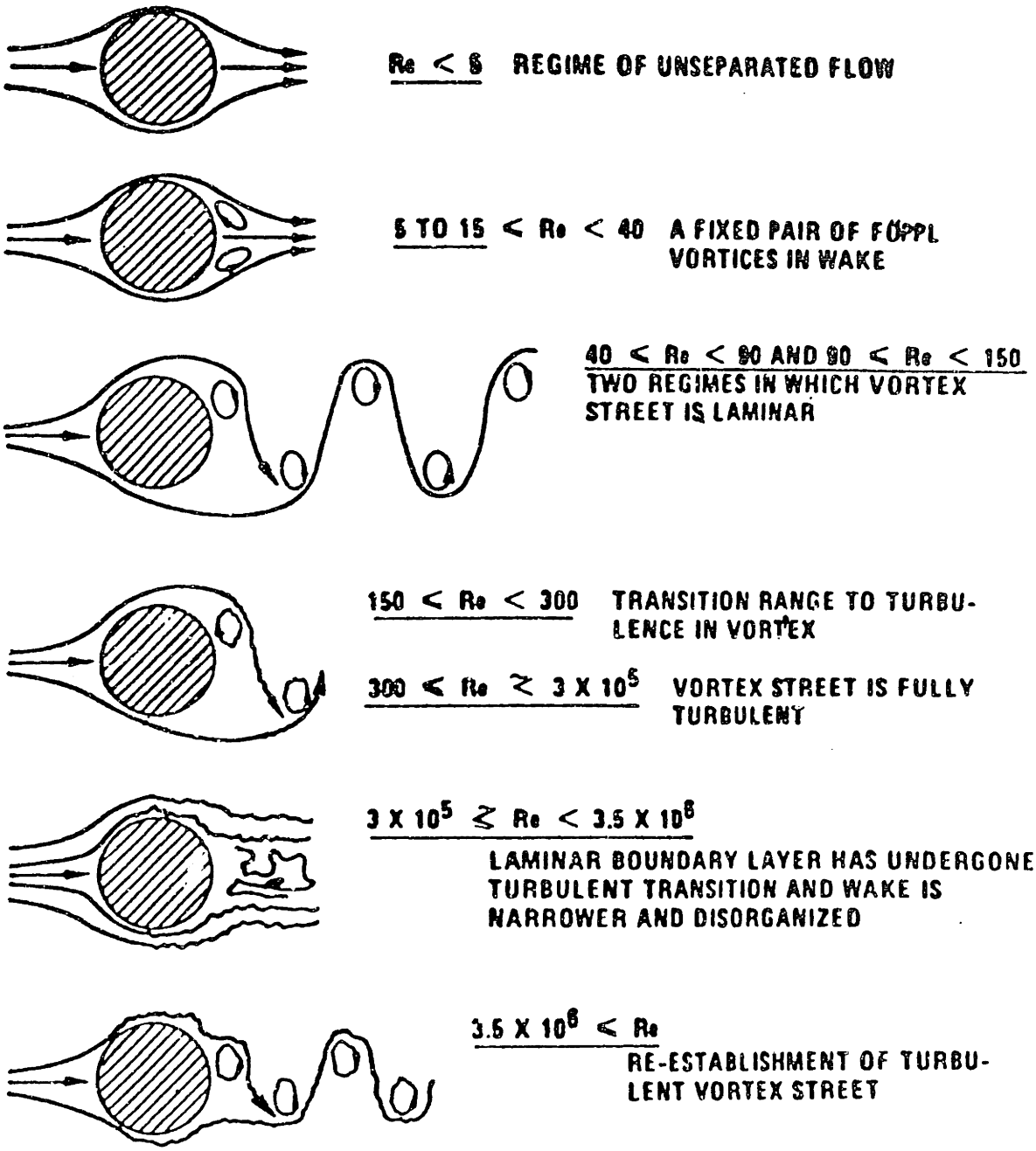

Figure 2.1: Regimes of fluid flow across circular cylinders

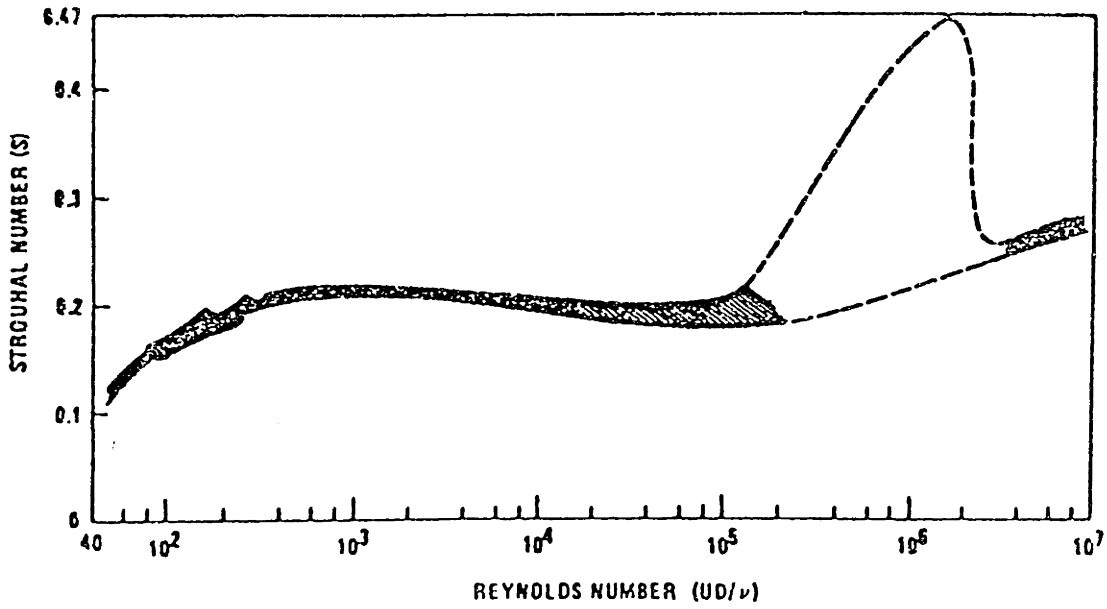

Figure 2.2: Reynolds number dependency of the Strouhal number for circular cylinders

2.2 Effects of Cylinder Motion in a Uniform Flow

All marine cables have some degree of flexibility and will oscillate under the effects of vortex shedding. It has been shown that the cables own motion directly effects the vortex shedding process, hydrodynamic damping and overall cable dynamics. An important hydrodynamic phenomena related to cylinder motion is that of lockin. Lockin occurs when the frequency of motion and fi quency of vortex shedding are synchronized. When synchronized there is a decrease in damping and a corresponding increase in dynamic response. This concept will be developed further in chapter four.

The response of cylindrical structures in uniform flows is characterized by a broad lockin bandwidth. This bandwidth depends primarily on the ratio of cylinder mass to displaced fluid mass and on the reduced velocity which is defined as $V/(f_n D)$, where V is the flow velocity, D is the cylinder diameter, and f_n is the natural frequency of the structure. The lockin bandwidth depends to a lesser extent on structural damping. For the purposes of calculating natural frequencies and reduced velocity an added mass coefficient of 1.0 is used in this thesis.

Chapter 3

Governing Equations

3.1 Forces

The governing equations are derived under the basic assumption that the cable motion is normal to the direction of fluid flow, and that the out of plane dynamic solution of the cable with respect to fluid flow can be decoupled from the in plane motion. The forces acting on a segment of cable (fig 3.1) can be decomposed into two basic areas, the weight, buoyancy and tension forces, and the fluid hydrodynamic forces.

3.1.1 Weight and Buoyancy

Hydrostatic Force

As shown in figure 3.1, the hydrostatic force is always perpendicular to the cable axis. To define an effective tension along the length of the cable it is convenient to add and subtract the corresponding hydrostatic forces acting on the cable as shown in figure (3.2). Then, by lumping together all the hydrostatic forces pointing towards the interior of the cable element, we obtain the buoyancy force normal to the cable element as;

$$B = B_o[\cos\phi + s\frac{d\phi}{ds}]ds \tag{3.1}$$

where $B_o = \rho_w \cdot g \cdot A$, P_1 and P_2 are the hydrostatic pressures acting on the segment ends, ρ_w is the mass density of water, A is the cable cross-sectional area, and ds is the cable segment length.

Weight

It is possible to define the weight acting on a segment of cable, ds, as

$$W = mg(-\cos\phi\hat{n} - \sin\phi\hat{t})ds \tag{3.2}$$

Having defined the buoyancy force it is now also possible to define a net weight per unit length in water. We assume for simplicity that the volume per unit length of the cable is constant. For the vertical cable configuration of figure 3.3 the weight per unit unstretched length in the fluid,w, can be written as,

$$w = m \cdot g - \rho_w \cdot A \cdot g \tag{3.3}$$

Tension

In specifying tension we would like to include the spatially varying effects of buoyancy and weight. This results in a spatially varying tension $T(s)$ whose vertical component can be specified by a constant tension component added to a spatially varying component such that

$$T_v(s) = T_c + w \cdot s \tag{3.4}$$

where s is the length along the cable with its origin at the cable bottom and w is the weight per unit length in water defined previously.

Given the vertical cable configuration of figure 3.3 we see that the spatially varying tension, T(s), is made up of a constant tension component T_c defined at $s = 0$ and a spatially varying part which varies as the weight per unit length in the fluid w.

3.1.2 Hydrodynamic Forces

Fluid Drag force

To obtain the drag force, the separation principle is used. The drag force on a cylinder element ds in length is separated into a normal drag component , proportional to the square of the relative normal velocity and a tangential drag, proportional to the

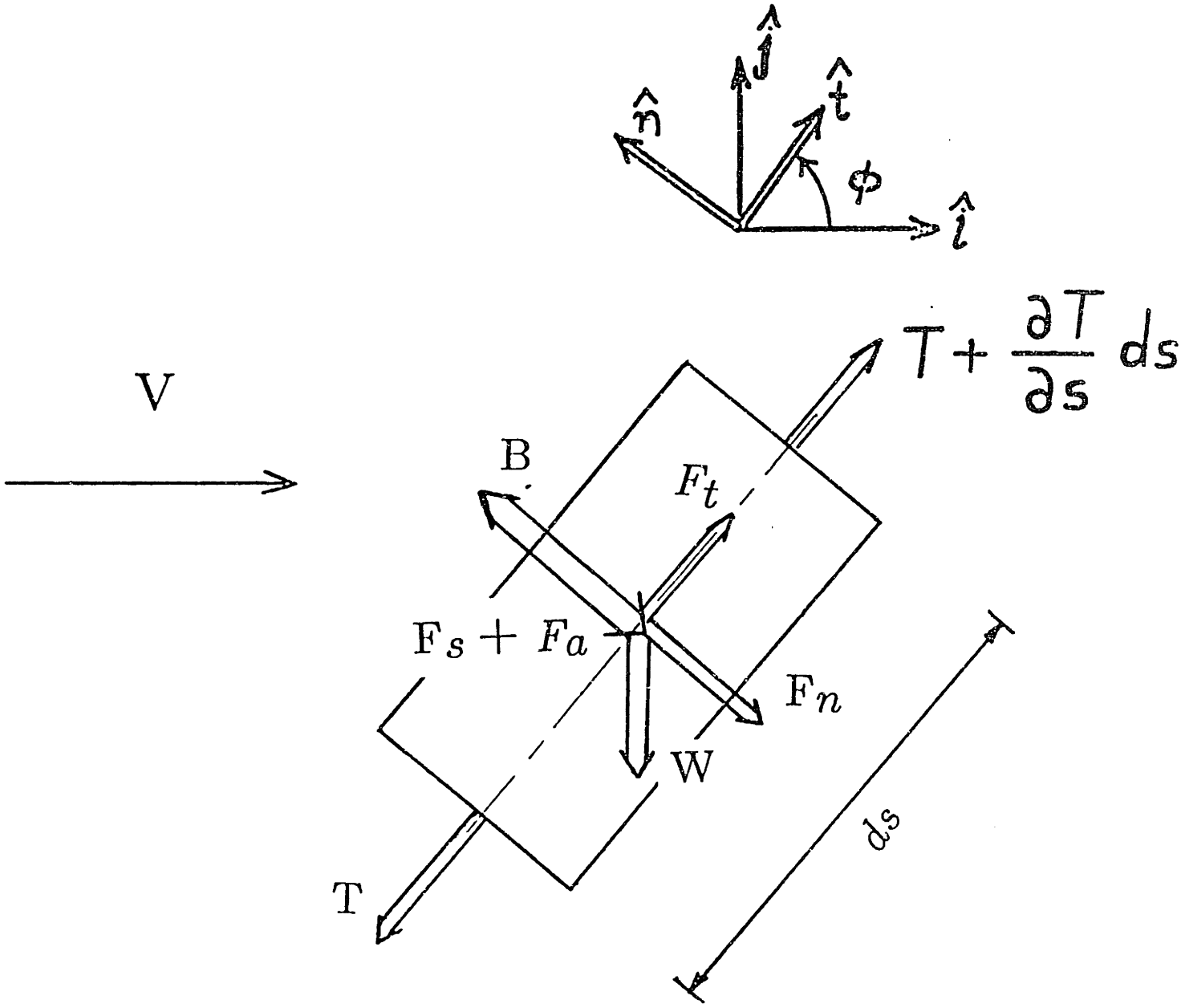

Figure 3.1: Forces acting on cable element

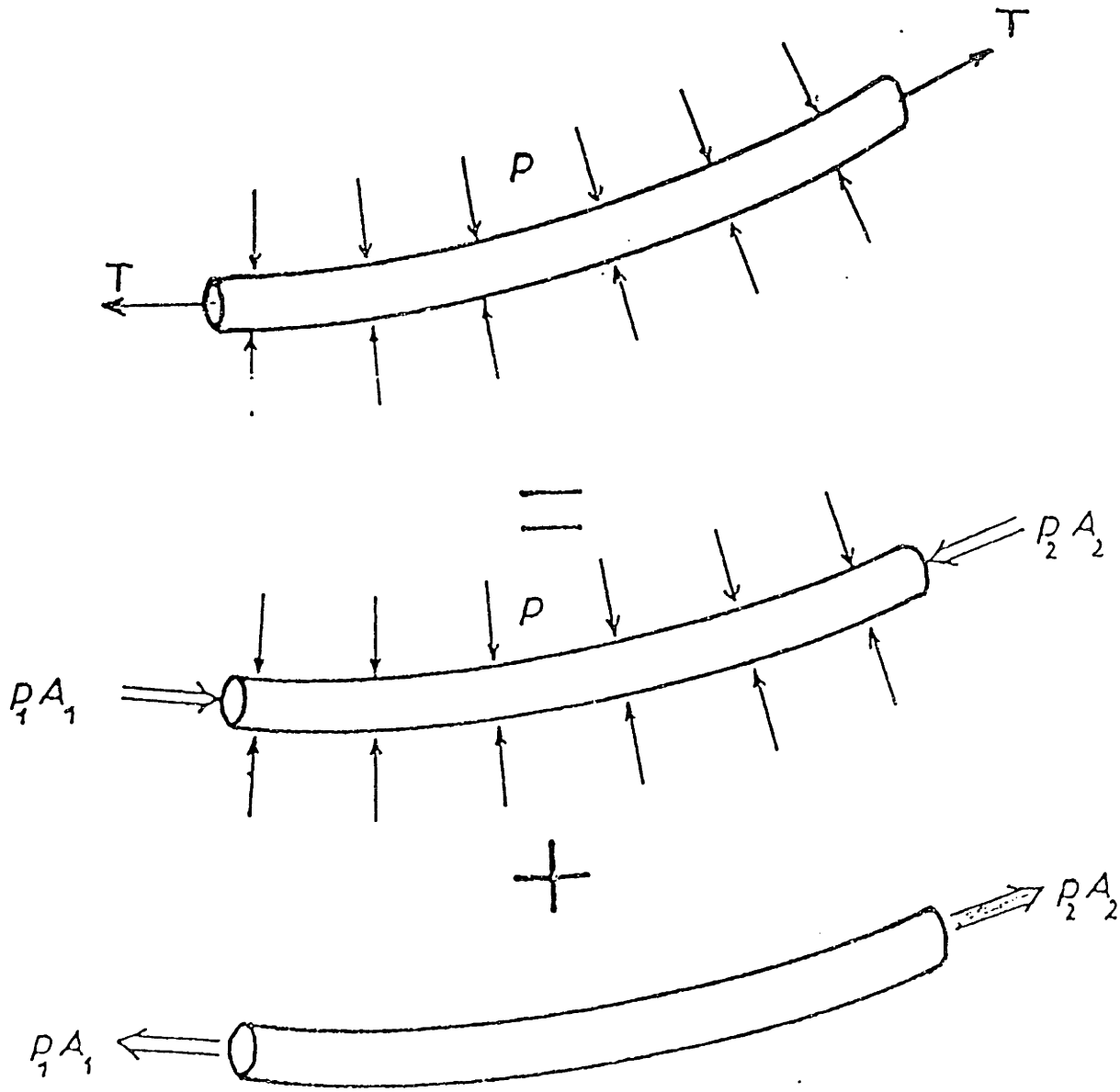

Figure 3.2: Hydrostatic forces

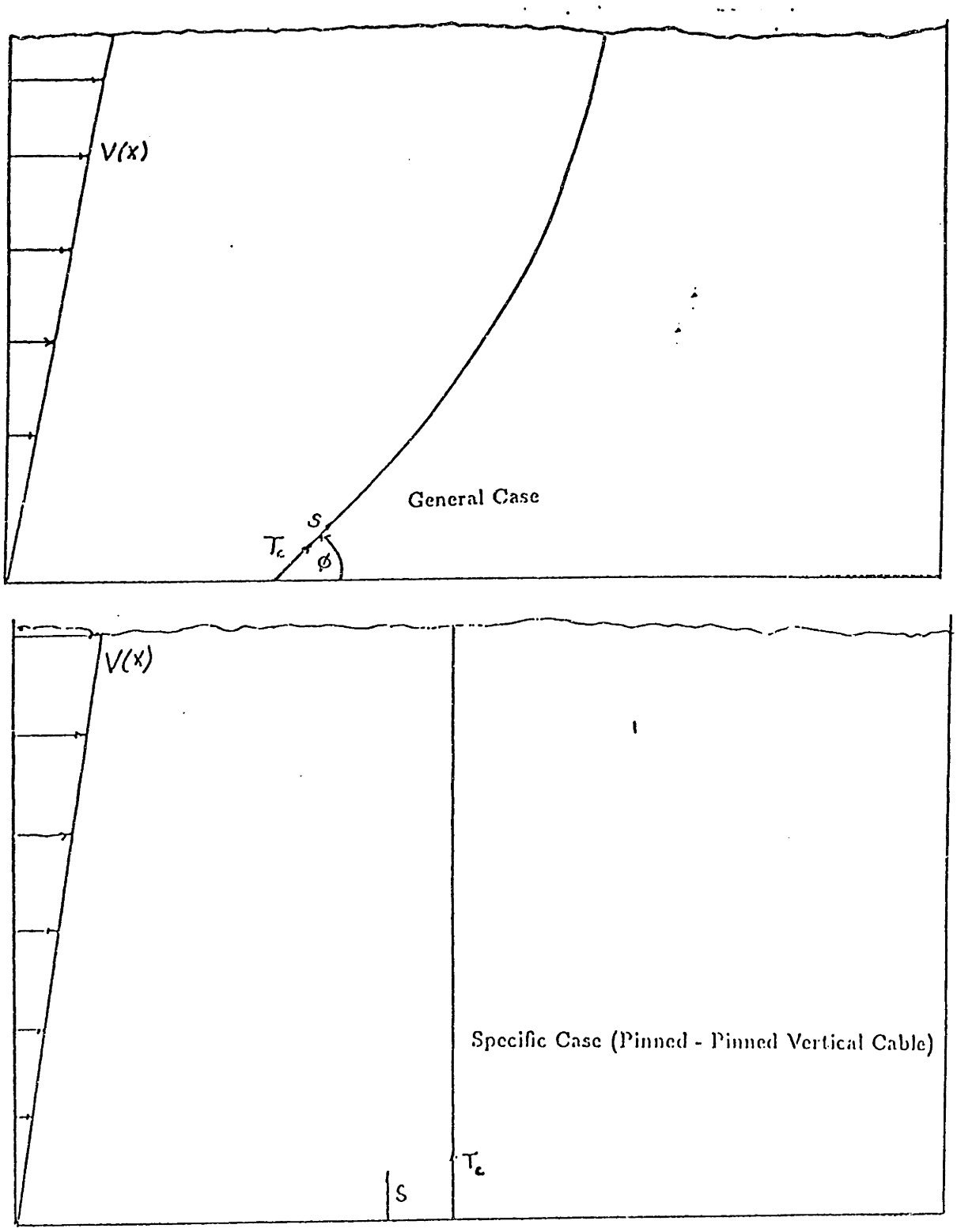

Figure 3.3: Cable configuration

square of the relative tangential velocity.

(i) The tangential drag on a segment ds is,

$$F_t = \frac{1}{2}\rho C_{dt}\pi D v_{rt}|v_{rt}|ds \;\; \hat{t} \tag{3.5}$$

Where v_{rt} is the relative velocity of the cable with respect to the flow in the $\hat{t}$ direction.

(ii) The normal drag on a segment ds is,

$$F_n = -\frac{1}{2}\rho C_{dn} D v_{rn}|v_{rn}|ds \;\; \hat{n} \tag{3.6}$$

Where v_{rn} is the relative velocity of the cable with respect to the flow in the $\hat{n}$ direction.

Structural Damping Force

The force on an element ds is modelled as a linear function of the local velocity of the cable.

$$F_s = -r_s \cdot v_n \cdot ds \tag{3.7}$$

where r_s is the linear structural damping constant per unit length.

Inertia Force

In addition to the drag force, the cable is subject to a fluid force which involves a fluid inertia component related to the added mass, m_a. The added mass for cables in the presence of currents has been the subject of much research (Lighthill),(Lenskii). It is known that many factors effect the value of added mass for a cylinder in a current, among these being the vortex shedding process, separation and cable vibration frequency. For simplicity, it is suggested that the added mass force on the element in the direction normal to the cable is given as:

$$F_a = -m_a \frac{\partial v_n}{\partial t} ds \tag{3.8}$$

and it is assumed that $m_a = \frac{\pi}{4}\rho D^2$, where D is the diameter of the cable in feet.

3.2 Governing Equations

The general form of governing differential equation for transverse motions of the cable can be written as,

$$M\frac{\partial^2 y}{\partial t^2} + C\frac{\partial y}{\partial t} - T\frac{\partial^2 y}{\partial s^2} - \frac{\partial T}{\partial s}\frac{\partial y}{\partial s} = f(s,t) \tag{3.9}$$

where y is the cable deflection in the $\hat{n}$ direction.

To arrive at a solution of the governing equations it is necessary to make several assumptions. The first is that the ratio of the wave speed of the elastic or longitudinal waves is large compared to that of the transverse waves. This is valid for most cable applications where the amount of cable stretching is small. The elastic wave speed is typically 20 times larger than the transverse wave speed. It can then be assumed that the solution consists of a part which is fast oscillating in space associated with transverse out of plane motions and a part which is slowly oscillating in space associated with the elastic wave motions.

The two solutions indicate corresponding physical mechanisms of dynamic behavior of the cable. The cable can either oscillate in the form of a taut wire (fast solution) around the static solution with small tangential displacements, or it can oscillate by changing the static configuration (slow solution) causing significant tangential displacements. For the case of vortex shedding phenomena we are concerned with the fast out of plane motions of the cable.

The second assumption is that the static quantities involved are slowly varying in space compared to the transverse oscillations. It turns out that this is typically true for the case of flow induced vibration. Under these conditions the governing equations can be written in non-dimensional form as [4];

$$\frac{-mL^2\omega^2 q}{T_c} = \frac{dT_1}{d\sigma} - \frac{wL}{T_c}\cos\phi_o\phi_1 \tag{3.10}$$

$$\frac{-(m+m_a)L^2\omega^2 p}{T_c} = T_1\frac{d\phi_o}{d\sigma} - \frac{d\phi_1}{d\sigma}\frac{T_o}{T_c} + \frac{wL}{T_c}\sin\phi_o\phi_1 \tag{3.11}$$

where;

T_c:Non varying static tension (defined at cable anchor)

$T_o(\sigma)$: Equilibrium tension of static configuration (Stretched condition), where $\frac{dT}{d\sigma} = wL\sin\phi_o$

$T_1(\sigma)$: Spatially varying dynamic tension component

ϕ: Angle between cable and horizontal

ϕ_o: Static component of ϕ

ϕ_1: Dynamic component of ϕ

s : Length along cable

σ: Non-dimensional Lagrangian coordinate, (s/L)

q : Non-dimensional tangential displacement, (x/L) $\hat{t}$ direction

p : Non-dimensional normal displacement, (y/L) $\hat{n}$ direction

Regarding tension variation, the dynamic component, $T_1(\sigma)$, is a second order effect resulting from cable strain. Since we are not concerned with the dynamic streching characteristics of the cable this force can be neglected. We will be concerned only with the static component of variation, $T_o(\sigma)$ which is dependent on cable mass and buoyancy per unit length.

The transverse equation for a string with variable tension is given by:

$$M(s)\frac{\partial^2 y}{\partial t^2} = \frac{\partial}{\partial s}[T_o(s)\frac{\partial y}{\partial s}] \tag{3.12}$$

Non-dimensionalizing the length variable, $\sigma = s/L$, and substituting $y = ye^{i\omega t}$ into 3.12 we obtain

$$\frac{d}{d\sigma}[T_o(\sigma)\frac{dy}{d\sigma}] + L^2M(\sigma)\omega^2 y = 0 \tag{3.13}$$

This equation is suitable to be solved using a WKB asymptotic analysis. For a detailed derivation see, [4], in which a WKB solution is used to solve 3.10 and 3.11. Then the leading order approximation expressed dimensionally for the fast out of plane dynamics of the cable,ignoring lift force excitation and damping, becomes:

$$y = \frac{1}{\sqrt[4]{T(s)/m_t}}[C_1e^{iW} + C_2e^{-iW}] \tag{3.14}$$

From this point on the subscript "o" will be dropped and the tension will be assumed to be a linear function of length along the cable which varies as weight per unit length in the fluid.

3.3 Natural Frequencies and Mode Shapes

This is the homogeneous solution for the fast out of plane dynamics of the cable. Applying the proper boundary conditions to these equations makes it possible to solve for the natural frequencies of the cable and to determine the corresponding mode shapes. Starting with the derived equation of motion,

$$y = \frac{1}{\sqrt[4]{T(s)/m_t}}[C_1e^{iW} + C_2e^{-iW}] \tag{3.15}$$

Where;

$T(s) = T_c + w{\cdot}s$

m_t = total mass per unit length, (m + m_a)

$W = \int_0^s \frac{\omega ds}{\sqrt{T(s)/m_t}}$

ω=frequency of vibration (rad/sec)

The simple case of a cable pinned at both ends has been chosen such that the boundary conditions are,

$$y(s=0)=0 \tag{3.16}$$

$$y(s=L)=0 \tag{3.17}$$

Satisfying the boundary condition at s=0 gives,

$$y(s=0)=\frac{1}{\sqrt[4]{T(0)/m_t}}[C_1+C_2] \tag{3.18}$$

resulting in $C_1=-C_2$.

Using this result and applying the second boundary condition at s=L gives,

$$y(s=L)=\frac{1}{\sqrt[4]{T(L)/m_t}}\sin\int_0^L\frac{\omega ds}{\sqrt{T(s)/m_t}}=0 \tag{3.19}$$

To satisfy zero displacement at s=L

$$\sin[\int_0^L\frac{\omega ds}{\sqrt{T(s)/m_t}}]=0 \tag{3.20}$$

$$\int_0^L\frac{\omega ds}{\sqrt{T(s)/m_t}}=n\pi \tag{3.21}$$

Evaluating this integral results in,

$$n\pi=\omega_n\frac{2}{w}\sqrt{m_t}[(T_c+w\cdot L)^{1/2}-(T_c)^{1/2}] \tag{3.22}$$

And from this the natural frequencies are found to be,

$$\omega_n=\frac{n\pi}{\frac{2}{w}\sqrt{m_t}[(T_c+w\cdot L)^{1/2}-(T_c)^{1/2}]} \tag{3.23}$$

From the previous results the characteristic mode shapes are found to be,

$$\phi_n = \sin \int_0^s \frac{\omega_n ds}{\sqrt{T(s)/m_t}} \tag{3.24}$$

$$\phi_n = \sin[\omega_n \frac{2}{w} \sqrt{m_t}[(T_c + w \cdot s)^{1/2} - (T_c)^{1/2}]] \tag{3.25}$$

Experiments have been conducted on a 57 foot long cable under a constant tension of 349 pounds and the resulting natural frequencies and response spectrums were measured [1]. The same cable properties will be used, only taking into account spatially varying tension. For the case of linearly varying tension we test two cases for different values of tension variation, w. For the first case, w was chosen to be 1.0 Lbs./ft. and T_c was 349 Lbs. For the chosen cable length of 57.3 feet this resulted in a tension variation from 349 pounds at the cable anchor to 406 pounds at the surface, an increase of 16.4 percent. The fundamental frequency obtained for this case was 0.96 Hz.

We next chose a tension variation value of 0.1 Lbs./ft. which resulted in a tension ranging from 349 pounds to 355 pounds. The resulting fundamental natural frequency was found to be 0.92 Hz. One would expect that for such a small tension variation the natural frequency would approach that of the constant tension case. The corresponding value for a constant tension cable of 349 pounds also 57 feet long was 0.92 Hz. We see that for a low tension variation factor the linearly varying tension value of natural frequency corresponds to that of the constant tension case. From this we can assume that the natural frequency and mode shape models derived for the linearly varying tension cable are accurate.

Chapter 4

Hydrodynamic Damping Model

In a sheared flow, the vortex shedding process excites the cable through a complex interaction. To describe the dynamic response of the system an accurate damping model is needed. The prediction model should be such that at any particular location the lift force should have a band limited spectrum centered on the dominant local vortex shedding frequency. This local spectrum is correlated to the force at neighboring locations through a parameter known as the correlation length, L_c. For details on the hydrodynamic damping of flexible cylinders see [3].

The fluid damping forces acting on the cable come about as a result of the free stream velocity, V, and the cross-flow cable velocity, $\dot{y}$. A damping force per unit length can then be assumed to be proportional to the relative velocity squared, fig.[4.1].

$$F_D = \frac{1}{2}\rho_w C_D D(V^2 + \dot{y}^2) \tag{4.1}$$

and the component of force in the y direction becomes,

$$F_y = -G\dot{y}\sqrt{V^2 + \dot{y}^2} \tag{4.2}$$

where $G = \frac{1}{2}\rho_w C_D D$ and D is the diameter of the cable. The damping force given above is a non-linear function of $\dot{y}$. It is convenient to find a linear equivalent damping constant such that the dissipative force may be expressed as

$$F_{y1} = -R(x)\dot{y} \tag{4.3}$$

Where F_{y1} and F_y are not necessarily equal and R(x) is is the equivalent hydrodynamic damping constant per unit length.

An estimate can be obtained for the linear equivalent damping constant , R(x),for harmonic oscillations by equating the energy lost per cycle of the non-linear damping force to that of the equivalent linear damping force. The expression for energy dissipated per cycle can be written as,

$$E_{dis} = \int_0^{\frac{2\pi}{\omega_o}} \Pi_{dis}(t)dt \tag{4.4}$$

$$= \int_0^{\frac{2\pi}{\omega_o}} F_D \cdot \dot{y} dt \tag{4.5}$$

$$= \int_0^{\frac{2\pi}{\omega_o}} R(x)\dot{y}^2 dt \tag{4.6}$$

$$= 2\int_0^{\frac{\pi}{\omega_o}} G\dot{y}^2\sqrt{V^2 + \dot{y}^2}dt \tag{4.7}$$

For values of $|\dot{y}^2| \leq \frac{V^2(x)}{2}$ the linear equivalent damping takes the form,

$$R(x) = GV[1 + \frac{3}{8}|\frac{\dot{y}^2}{V^2}|] \tag{4.8}$$

$$= \gamma GV(x) \tag{4.9}$$

where γ is a factor to account for the cables own motion, $\dot{y}$, and varies from 1.0 to 1.3. Technically, the value of γ should also be a function of x because $\dot{y}$ is a function of x. For the sake of simplifying the damping estimate, though, we have chosen a lower bound value for γ of 1.0. More serious errors occur in attempting to partition the cable into forced and damped regions.

This is a common way of describing fluid drag forces acting on bodies. This model, however, does not take into account the effect the vortex shedding process itself has on the motion. In regions for which the vortex shedding and cylinder motion are found to be correlated power flows into the system. In the power-in region the vortex- induced exciting forces are in phase with the cable velocity, $\dot{y}$. Portions of the cable where the lift force is uncorrelated to the cable velocity results in a damping region. The damping model must be able to distinguish between these regions both as a function

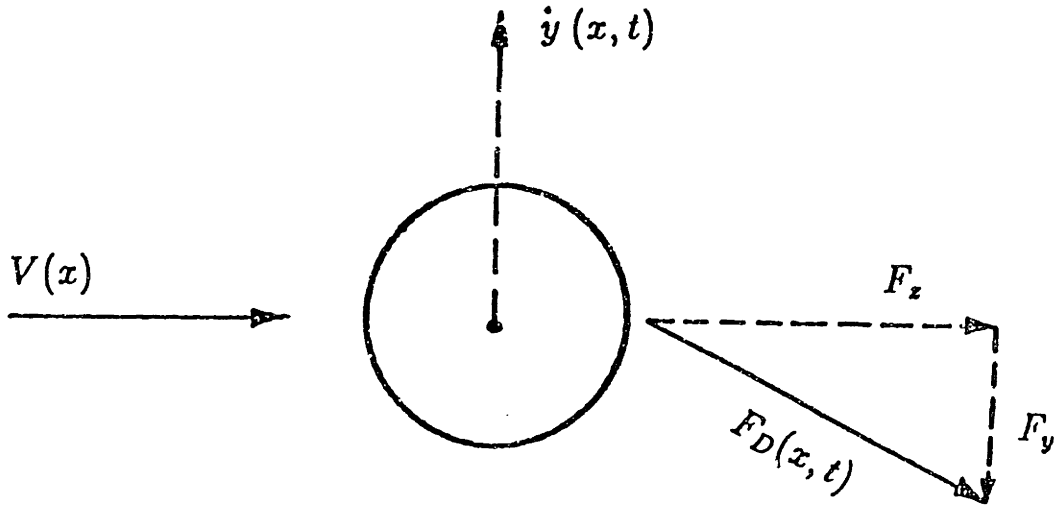

Figure 4.1: Drag force vector decomposition

of frequency and location.

Damping for a Finite Length Cable

For short cylinders excited in their low modes it is appropriate to calculate the individual modal damping constants and damping ratios. The linear equivalent modal damping constant, $R_{h,n}$, is calculated as,

$$R_{h,n} = \int R(x)\phi_n{}^2(x)dx \tag{4.10}$$

The mode shapes ϕ_n have already been calculated as,

$$\phi_n = \sin[\mu_n m_t{}^{1/2}\frac{2}{w}[(T_c + w{\cdot}s)^{1/2} - (T_c)^{1/2}]] \tag{4.11}$$

$$\phi_n{}^2 = \sin^2[\mu_n m_t{}^{1/2}\frac{2}{w}(T_c + w{\cdot}s)^{1/2} - \mu_n m_t{}^{1/2}\frac{2}{w}(T_c)^{1/2}] \tag{4.12}$$

$$= \frac{1 - \cos[2\mu_n m_t{}^{1/2}\frac{2}{w}(T_c + w{\cdot}s)^{1/2} - 2\mu_n m_t{}^{1/2}\frac{2}{w}(T_c)^{1/2}]}{2} \tag{4.13}$$

$$= \frac{1}{2} - [\frac{\cos(u)\cos(v) + \sin(u)\sin(v)}{2}] \tag{4.14}$$

Where,

$$u = 2\mu_n m_t{}^{1/2}\tfrac{2}{w}(T_c + w{\cdot}s)^{1/2}$$

$$v = 2\mu_n m_t{}^{1/2}\tfrac{2}{w}(T_c)^{1/2}$$

Now $R_{h,n}$ can be calculated. However, this modal damping constant does not, as yet, account for the power-in, power- out regions discussed previously. To account for this effect the corellation length must be incorporated as a limit in the integration. To accomplish this we define,

$$(R_{h,n})_{max} = \int_0^L R(x)\phi_n{}^2 dx \tag{4.15}$$

For the case of a sheared flow a more accurate model for modal damping is,

$$R_{h,n} = H(R_{h,n})_{max}, \tag{4.16}$$

where the coefficient H is defined as,

$$H = \frac{\int_0^{x_n - L_c} V(x)\phi_n{}^2(x)dx + \int_{x_n+L_c}^{L} V(x)\phi_n{}^2(x)dx}{\int_0^L V(x)\phi_n{}^2(x)dx}, \tag{4.17}$$

where $H \leq 1$ for all cases and x_n is the most favorable location for a resonant condition to exist between the vortex shedding process and mode n. L_c is the correlation length which is the seperation distance that causes the excitation at two locations to drop below a specified value.

Now we may assume a shear velocity profile which increases linearly from zero to a maximum value such that $V(x) = V_p(\frac{x}{L})$, where V_p is the peak velocity in the shear. Given this relation we can now write,

$$R(x) = \gamma G V_p x/L \tag{4.18}$$

and by substitution into equations 4.15 and 4.16 the modal damping values can be calculated for the linear shear profile.

In the excitation model presented by Chung [1] the spatial cross-correlation of the lift force spectrum is probabilistically defined as a Gaussian random process with the correlation length as the standard deviation. Simply stated there is a portion of the cable $2L_c$ in length in which most of the power for mode n will flow into the system. Outside of this region will account for the dominant source of hydrodynamic damping for mode n.

Ramberg and Griffin measured wake velocity signals behind the vibrating flexible cables using hot wire anemometers in an open jet wind tunnel and they calculated the cross-correlation coefficient of the wake velocity signals (Ramberg and Griffin). It was found that for the portion of a vibrating cable over which the vortex shedding

and vibration frequencies are locked together, the spatial cross-correlation coefficient between any two locations in the wake behind that portion approached unity, being limited only by turbulence. In this case, the correlation length in the excitation model will be infinite. However, in a sheared flow case several modes can be excited simultaneously by the flow and the correlation length should be finite. At two adjacent resonant locations, X_n and X_{n+1}, for the nth and (n+1)th mode, respectively, in a sheared flow the wake will not be significantly correlated.

The correlation length used here is the span corresponding to half the modal spacing in vortex shedding frequency. For the linear shear flows considered here the correlation length coefficient, l_c, is specified as;

$$l_c = \frac{L_c}{L} \simeq \frac{1}{2N} \tag{4.19}$$

where;

L_c = the correlation length

L = the cylinder length

N = the number of modes excited by the sheared flow

For very long cables in sheared flows where N is very large, the ratio of the power-in region for each mode to total cylinder length, $2L_c/L$, will be very small and $H \simeq 1$.

It is now possible to relate the linear equivalent modal damping constant to the corresponding modal damping ratios.

$$\varsigma_{n,max} = \frac{R_{h,n,max}}{2\omega_n M_n}, \tag{4.20}$$

Where M_n is the modal mass defined as $\frac{m_t L}{2}$

$$\varsigma_n = H_n \varsigma_{n,max} \tag{4.21}$$

If for the moment we assume a constant tension acting on the cable then it is possible to simplify the relation for ς_n. For the constant tension cable the following

relations can be written,

$$\phi = \sin \frac{n\pi x}{L} \tag{4.22}$$

$$G = \frac{1}{2}\rho_w C_D D \tag{4.23}$$

$$R(x) = \gamma G V_p \frac{x}{L} \tag{4.24}$$

$$R_n = \int_0^L R(x)\phi_n{}^2(x)dx \tag{4.25}$$

$$\varsigma_n = \frac{R_n}{2\omega_n M_n} \tag{4.26}$$

$$= \frac{\gamma C_D V_r(\omega_p/\omega_n)}{4\pi^2(sg + C_a)} \tag{4.27}$$

V_r ; Reduced velocity

ω_p ; Peak excitation frequency

If a low value of tension variation is substituted into equation 4.15 then that result can be seen to approach the corresponding values obtained from 4.27.

Chapter 5

Response Prediction Model

An accurate response prediction model consists of four basic elements: a structural model, a damping model, an excitation force model, and a solution technique. The structural model and hydrodynamic damping model have already been presented, and the excitation force model is that which was developed by T.Y. Chung [1]. In this chapter a response prediction method is proposed for the vortex-induced vibration of a non-constant tension cable in a sheared flow based on a Green's function approach.

Vortex induced vibration of long cylinders in uniform flows can be predicted well on the basis of experimental data. For the case of a cylinder in a shear flow a mode superposition approach is often used. The amplitude of each mode is determined using information from experimental results in uniform flows. Under the assumption of small damping, the total response amplitude is obtained by sum of squares superposition of resonant modes. This model, however, cannot account for spatial attenuation observed in the response in highly sheared flows where non-resonant modes become important in the total response. The mode superposition response model must use the non-resonant modes to accurately predict the response. If the Green's function is available it gives more accurate and efficient results because it is equivalent to summing an infinite number of modes.

Equation 3.15, which has been used to solve for the system natural frequencies and mode shapes, constitutes the homogeneous linear dynamic equation. The vortex-shedding related forces constitute the inhomogeneous terms of the equations of mo-

tion. Equations [3.9,10,11] can be used to construct the system Green's function which will provide the forced dynamic response.

The general form of the Green's function is found to be [2]

$$G(s,x) = \frac{\sinh \int_0^s \frac{i\mu ds}{\sqrt{T(s)/m_t}} \sinh \int_x^l \frac{i\mu ds}{\sqrt{T(s)/m_t}}}{i\mu\sqrt{m_t}\sqrt[4]{T(s)T(x)} \sinh \int_0^l \frac{i\mu ds}{\sqrt{T(s)/m_t}}} \quad 0 \leq s < x \tag{5.1}$$

$$G(s,x) = \frac{\sinh \int_s^l \frac{i\mu ds}{\sqrt{T(s)/m_t}} \sinh \int_0^x \frac{i\mu ds}{\sqrt{T(s)/m_t}}}{i\mu\sqrt{m_t}\sqrt[4]{T(s)T(x)} \sinh \int_0^l \frac{i\mu ds}{\sqrt{T(s)/m_t}}} \quad x \leq s \leq l \tag{5.2}$$

In a linear one dimensional continuous system the displacement response spectrum at a location may be determined from the following integral equation;

$$S_{yy}(s,\omega) = \int_0^L dx \int_0^L dx' S_{fxfx'}(x,x',\omega) G(s,x) G^*(s,x') \tag{5.3}$$

$S_{yy}(s,\omega)$; Displacement response spectrum at location s

$S_{fxfx'}(x,x',\omega)$; Lift force spectrum

G(s,x); Green's function due to an excitation at the point s = x

$G^*(s,x')$; Conjugate of the Green's function due to an excitation at the point s = x'

If the Green's function is solved for the case of no damping and a linearly varying tension is substituted into the expressions we obtain a purely real solution of,

$$G(s,x) = \frac{\sin B \sin C}{\sin A} \frac{1}{\omega\sqrt{m_t}\sqrt[4]{T(s)T(x)}} \quad 0 \leq s < x \tag{5.4}$$

$$G(s,x) = \frac{\sin D \sin E}{\sin A} \frac{1}{\omega\sqrt{m_t}\sqrt[4]{T(s)T(x)}} \quad x \leq s \leq L \tag{5.5}$$

$$A = \omega\sqrt{m_t}\tfrac{2}{w}[(T_c + w{\cdot}L)^{1/2} - (T_c)^{1/2}]$$

$$B = \omega\sqrt{m_t}\tfrac{2}{w}[(T_c + w{\cdot}s)^{1/2} - (T_c)^{1/2}]$$

$$C = \omega\sqrt{m_t}\tfrac{2}{w}[(T_c + w{\cdot}L)^{1/2} - (T_c + w{\cdot}x)^{1/2}]$$

$$D = \omega\sqrt{m_t}\tfrac{2}{w}[(T_c + w{\cdot}x)^{1/2} - (T_c)^{1/2}]$$

$$E = \omega\sqrt{m_i}\frac{2}{w}[(T_c + w{\cdot}L)^{1/2} - (T_c + w{\cdot}s)^{1/2}]$$

We see that this results in a pure sinusoid, and one would expect the response shape to match that of the characteristic mode shapes, which is the case.

For our case it is necessary to account for damping, and this is accomplished by incorporating the damping within the complex frequency which is defined as,

$$\mu^2 = \omega^2 - \frac{i\omega(r + r_s)}{(m + m_a)} \tag{5.6}$$

ω; Real frequency

r; Hydrodynamic damping constant

r_s; Structural damping constant

m; Structural mass per unit length

m_a; Added mass per unit length

Taking into account the system damping requires expanding the Green function into its real and imaginary components to make it possible to perform the necessary numerical integration. This expansion results in a complex equation involving the hyperbolic cosine and tangent functions. The tanh is a numerically stable function, however the hyperbolic cosine function becomes numerically unstable for large arguments. Therefore, it is necessary to manipulate the Green's function into the form below in order to minimize numerical inaccuracies due to the hyperbolic functions. The real and imaginary components of the Green's function then become,

$$GR(s,x) = \frac{\cosh(q2)}{\cosh(q1)}\cosh(q3)C_1 \tag{5.7}$$

$$GI(s,x) = \frac{\cosh(q2)}{\cosh(q1)}\cosh(q3)C_2 \quad 0 \leq s < x \tag{5.8}$$

$$GR(s,x) = \frac{\cosh(q4)}{\cosh(q1)}\cosh(q5)C_3 \tag{5.9}$$

$$GI(s,x) = \frac{\cosh(q4)}{\cosh(q1)}\cosh(q5)C_4 \quad x \leq s \leq L \tag{5.10}$$

Where q1, q2, q3, q4, and q5 result from an expansion of the complex frequency, μ,(see Appendix A). And C_1 ,C_2, C_3 and C_4 are composed of all terms not involving the hyperbolic cosine.

It is interesting to investigate the behavior of the Green's function for different modes and different values of damping and compare these values to the corresponding results for the constant tension cable. We choose a small tension variation, $(w = 0.1)$, such that for equivalent damping and frequency conditions the linearly varying tension Greens function approaches the corresponding constant tension Green's function.

We first examine the case of very low damping for a frequency very close to the characteristic frequency of the third mode. We expect to see oscillatory behavior similar to the one obtained from the third characteristic mode shape determined previously. A damping ratio of 0.01 was chosen, and the cable was excited at $s = 0.5 \cdot L$ at a frequency very near that of the third mode natural frequency. From figure 5.1 we see that the corresponding Green function oscillates in a shape very near that of the third mode. This solution would be expected for the case of very low damping at a frequency near resonance. The next situation examined was that of a very high mode number with relatively high damping for the given mode; $(n = 100, \varsigma = 0.1)$. For this case we see a much greater attenuation in the shape of the Green's function for this highly damped case as well as a significant reduction in amplitude. The cable behaves as if it were infinite in length. The final case looked at was that of an intermediate mode number; $(n = 10, \varsigma = 0.1)$. See figures 5.1 - 5.3.

It was also interesting to see what effect a larger tension variation would have on the Green's function. Two cases were tested. The values of n and damping ratio were 10 and 0.1 respectively. Figure 5.4(a) corresponds to a linear tension variation of $w = 10$ Lbs/ft and figure 5.4(b) corresponds to a variation of 50 Lbs./ft. From these plots one can see that the Green's functions are no longer symmetric. The increased tension variation has effectively changed the phase speed c_p over the length of the cable. Therefore in portions of the cable where tension is greater it can be seen that

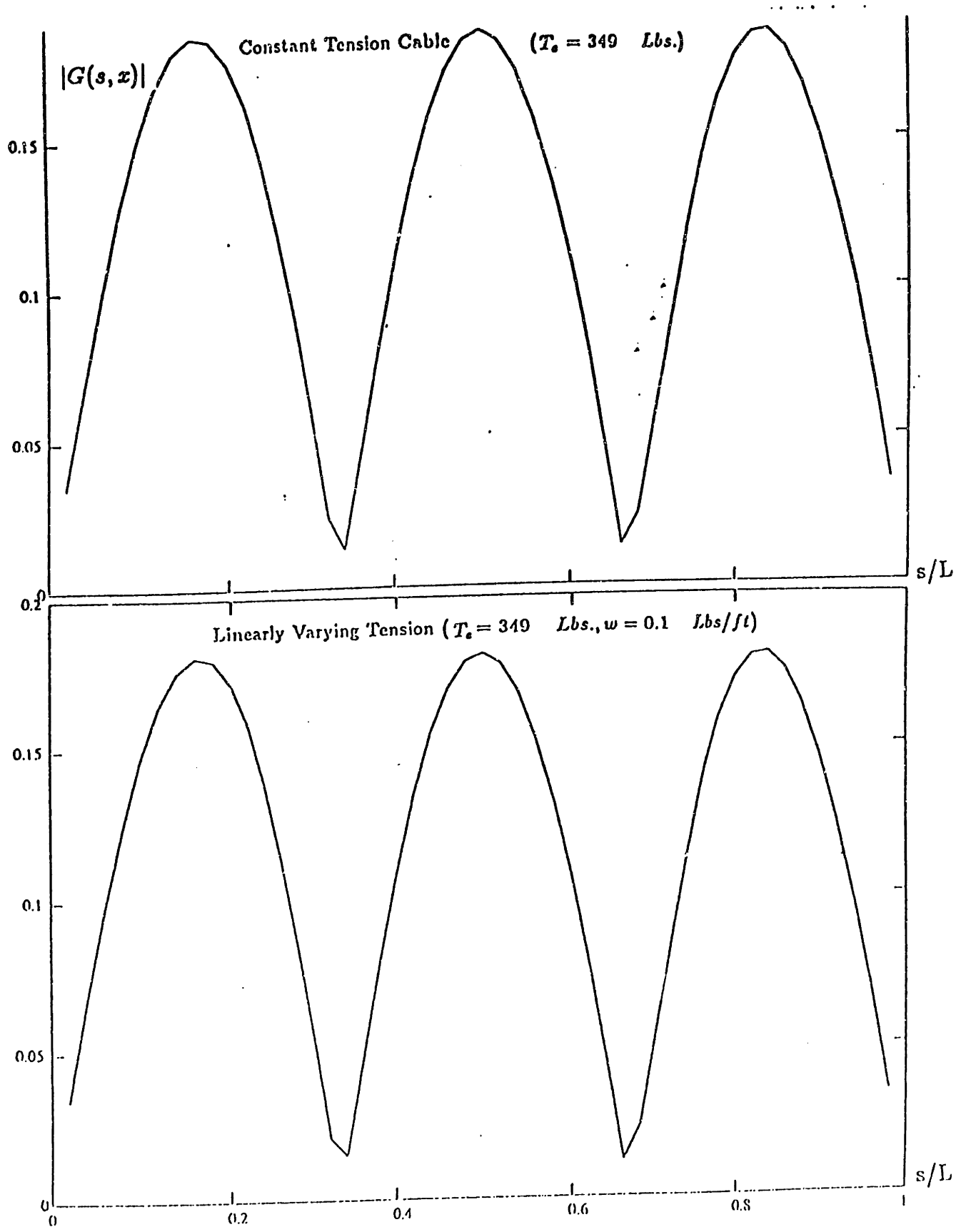

Figure 5.1: Greens function response ($n = 3, \zeta = 0.01$)

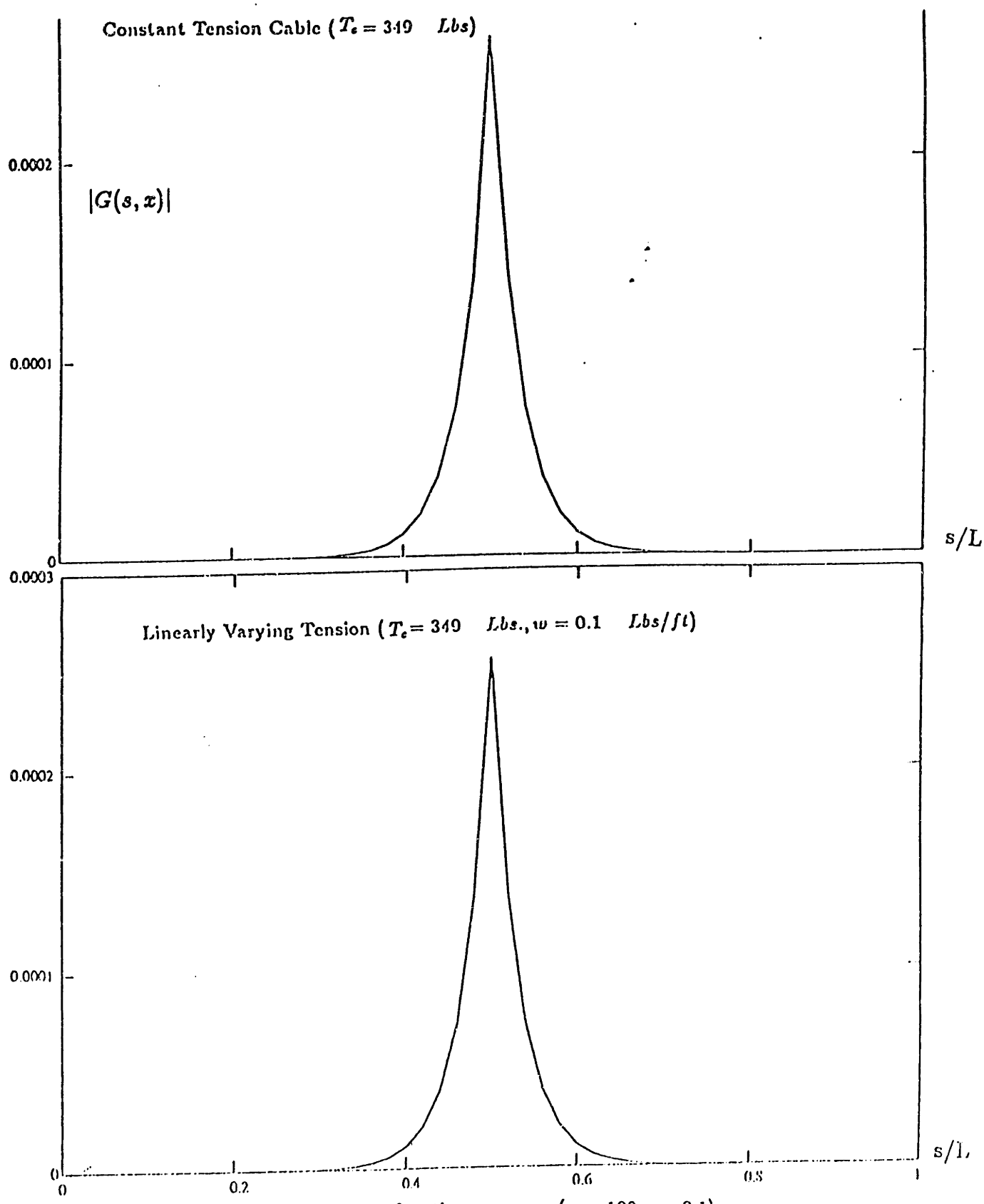

Figure 5.2: Greens function response ($n = 100, \zeta = 0.1$)

wave speed is also greater (i.e. λ is larger).

The Green's function magnitudes were ploted as a function of non- dimensional length along the cable, (s/L), for both slowly varying ($w = 0.1$) and constant tension cases and one can see that they match nearly exactly. Slight discrepancy would be due to the different way in which damping is used for the two different Green's functions.

The Greens function is an exact solution equivalent to summing an infinity of modes, but one would expect that for conditions near resonance the response of the system would be dominated by that particular resonant mode. This can be shown through a modal analysis technique whereby a unit force is applied at $s = 0.5 \cdot L$ and the response at this location is calculated and compared to the corresponding response obtained from the Green function. The modal analysis technique proceeds as follows.

First we use the separation of variables principle which provides a solution of the form

$$y(x,t) = \eta_n(t)\phi_n(x), \tag{5.11}$$

then the modal time response solution can be written as;

$$M_n\ddot{\eta}_n + C_n\dot{\eta}_n + K_n\eta_n = N_n(t) \tag{5.12}$$

Given a forcing function, $f(x,t) = \delta(x - L/2)e^{i\omega t}$, we can calculate the modal forcing term, $N_n(t)$, as;

$$\int_0^L f(x,t)\phi_n(x)dx \tag{5.13}$$

Substituting the previously described forcing function into this equation results in,

$$N_n(t) = e^{i\omega t}\int_0^L \delta(x - L/2)\phi_n(x)dx \tag{5.14}$$

$= e^{i\omega t}\phi_n(x = L/2)$

$= e^{i\omega t}$

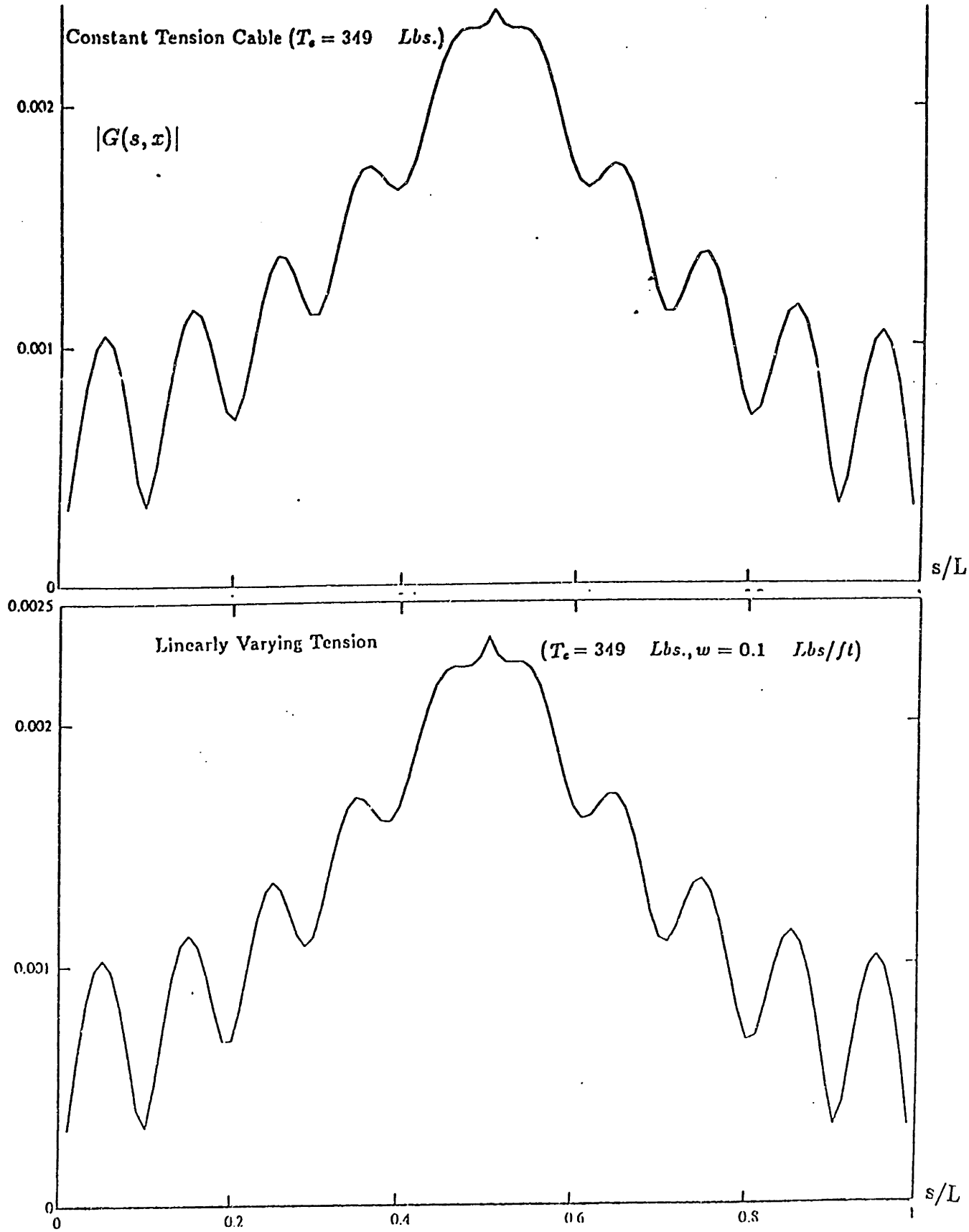

Figure 5.3: Greens function response ($n = 10, \varsigma = 0.1$)

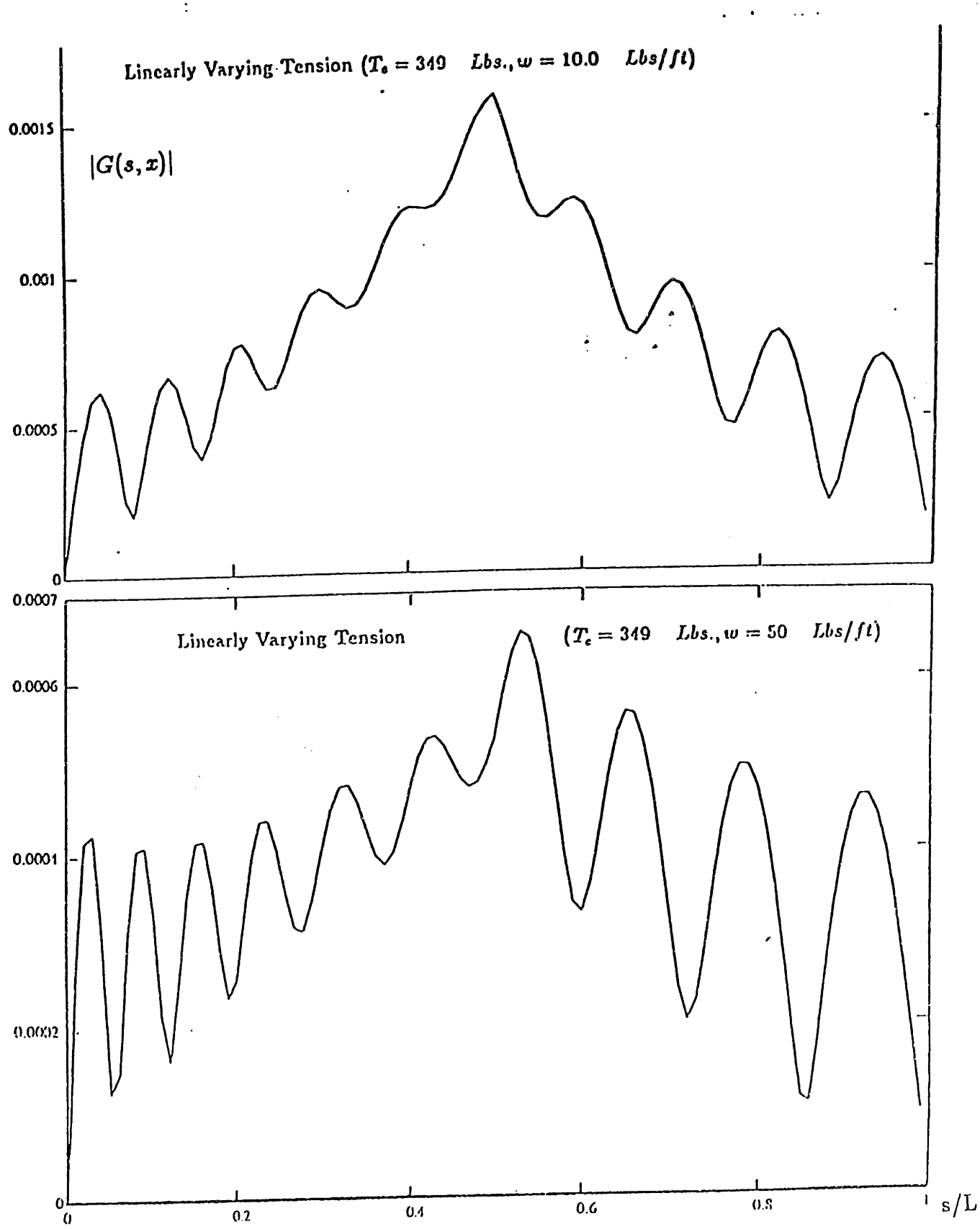

Figure 5.4: Greens function response ($n = 10, \varsigma = 0.1$)

The corresponding transfer function for this system can be written as

$$\frac{\eta}{N} = \frac{\frac{1}{K_n}}{\left[\left(1 - \frac{\omega}{\omega_n}^2\right)^2 + \left(2\zeta\frac{\omega}{\omega_n}\right)^2\right]^{1/2}} \tag{5.15}$$

Near resonance we know that $\omega \approx \omega_n$ and the resulting transfer function is;

$$\frac{\eta}{N} = \frac{\frac{1}{K_n}}{2\zeta_n} \tag{5.16}$$

And finally by substituting values for modal stiffness and modal forcing function into this relation we obtain;

$$|\eta_n| = \frac{1}{2M_n{\omega_n}^2\zeta_n} \tag{5.17}$$

Next, we do an example choosing to test the third mode case. Choosing corresponding values of natural frequency, modal mass, and damping ratio it is possible to compare the value from the above expression to the value of the magnitude of the Greens function when taken at third mode conditions.

Substituting the appropriate third mode parameters for the linearly varying tension cable, ($w = 0.1$), into the above relation yields a result of 0.027. The value obtained by substituting the same parameters into the non-constant tension Greens function was 0.0276. The constant tension cable was also tested for the same conditions. Third mode values of natural frequency and damping were substituted into the modal displacement expression resulting in a value of 0.027. Substituting the corresponding values into the constant tension Greens function resulted in a value of 0.0279. These values all corresponded to within 2 percent of each other. Therefore the non-constant tension Greens function can be assumed to be accurate for conditions near those of lightly damped resonant modes.

Having established the form of the non-constant tension Greens function it was interesting to see which parameters effected the Greens function for the linearly vary-

ing tension case and how changes in these parameters effected the magnitude of the resulting Greens function.

In examining the form of the Greens function, it was found that the parameters which it was mostly dependent on were the damping per unit length and tension variation. The tension variation coefficient which is dependent on weight per unit length in the fluid, cable length, and constant tension component, T_c, and is defined as,

$$\underline{a} = \frac{wL}{T_c} \tag{5.18}$$

We proceeded by first seeing what effect variation of tension coefficient would have on the magnitude of the Greens function. The coefficient was varied between 0.02 and 2.0 and all other parameters of the function (damping, frequency..) were held constant. It was seen that for values of $\underline{a}$ less than 0.2 the constant tension response and the linearly varying response were effectively the same. For values of $\underline{a}$ above about 0.2 the Greens function was seen to become asymmetric due to changes in phase velocity along the length of the cable, and the resulting response values for the linearly varying tension case began to differ significantly from those of the constant tension cable.

Next we examined the effect changes in damping had on the magnitude of the Greens function. The damping per unit length was allowed to vary while all other parameters (coefficient, frequency..) were held constant. This was done for frequencies close to those of the mainly excited modes, (1-4 for this case), and it was found that the Greens function dependency on damping was of the form of equation 5.17. The constant tension Greens function was see to be equally dependent on damping

For low coeffcients of tension variation ($\underline{a} < 0.2$) it has been shown that the Greens functions for the constant tension and linearly varying tension cases are essentially the same. From this, one would also expect that for the same small tension variation the corresponding response spectra for the constant tension versus linearly varying cases would also be equivalent.

A computer model has been developed which calculates response spectra for the linearly varying tension cable located in a sheared current profile. This computer model was used for the cable described in chapter three. Figures 5.5, 5.7 and 5.11 give the necessary computer input parameters for both the constant tension and linearly varying tension cases tested. The cable, which had dimensions of 57.3 feet in length and 1.125 inches in diameter, was located in a linear shear profile with velocities ranging from 0.0 ft/sec at s/L = 0.0 to 2.15 ft/sec at s/L = 1.0. The input parameters to the model include the physical properties of the cable, the velocity profile characteristics, as well as all necessary coefficients (drag, added mass, lift). The output (figures 5.6, 5.8 and 5.12) consists of the displacement and acceleration spectra for a specified response location as well as the rms displacement values for the given response point.

Several cases were examined for the above cable. In the first the tension variation was chosen to be very small. In doing this we attempt to show that for sufficiently small coefficient of variation the linearly varying tension cable can be treated as if it were under constant tension. The second case involves a greater tension variation for which we expect to see more significant changes in the response values of the linearly varying cable as compared to the constant tension case.

Figures 5.9 and 5.10 (a) and (b) are the displacement and acceleration spectra for the constant tension cable (a) and the linearly varying tension cable (b). The coefficient of tension variation for (b) was 0.02 and the constant tension components for both cases was 349.0 pounds. One can see from the respective displacement and acceleration spectra that if superimposed on one another they are effectively the same. For both the constant tension and linearly varying cases the mainly excited modes were found to be 1-4 which corresponded to mainly excited frequencies ranging from 0.92 to 3.71 Hz. From the spectra it is obvious that the total response is dominated by values in this frequency range , with the corresponding resonant peaks occuring at the natural frequencies for excited modes 1-4.

In the next case the tension variation was chosen such that it would effect the response of the linearly varying tension cable more significantly. When a tension variation coefficient of 0.82 ($w = 5.0 Lbs/ft$) was substituted into the model it was found that the mainly excited modes for the system were also 1-4, but the fundamental natural frequency increased to 1.084 Hz. as opposed to 0.92 for the constant tension cable. The resonant peaks were seen to shift accordingly (see figures 5.13 and 5.14) and the rms displacement at the corresponding location increased to 0.692 inches versus 0.587 for constant tension. This result shows that for tension variation coefficients above 0.2 the linearly varying component of tension plays a significant part in the total response.

Up until this point we have been comparing results from the linearly varying tension cable to the constant tension cable in an attempt to show that for low values of tension variation results for the non-constant tension cable would converge to the values obtained for the constant tension case. We found this to be true; values of natural frequency, damping, RMS displacement, and displacement and acceleration spectra for low tension variation ($\underline{a} < 0.2$) all were within 1 percent of the corresponding constant tension results. It was also shown that for coefficients of variation greater than 0.2 the linearly varying component of tension became significant in the response and the more complicated spatially varying tension model was necessary to accurately predict the response.

Now we would like to see how the model responds to a more practical application. The cables examined previously have been of relatively small dimensions (57 feet long, 1.125 inch diameter) and have only been excited in their first 4 - 6 modes. We now wish to examine the behavior of the more realistic situation of a linearly varying tension marine cable subjected to a shear current. The example is a 2000 foot long pipe with an outside diameter of 9.625 inches and an inside diameter of 8.375 inches.

These parameters resulted in a weight per unit length of 60.0 pounds per foot and a corresponding tension variation, (taking into account buoyancy), of 28.6 pounds per

```
0.25          frequency resolution in Hz. (delf)
100           no. of frequency points, fmax = np*delf
0.05          spacial resolution
57.25         cable length in feet, L
1.125         cable outside diameter in inches
62.4          density of the surrounding fluid in Lb/ft**3
0.5764        cable weight per foot in air in Lbs./ft.
1.0           added mass coefficient
349.          constant tension in Lbs.
0.17          Strouhal no.
2             Number of points specifying velocity profile
0.0,2.15      location(x/L), velocity(ft/sec) for first point
1.0,0.0       location and velocity for all succeding points
0.25          turbulence std deviation about mean velocity in ft./sec
0.003         structural modal damping ratio
1.0           drag coefficient
1.0           drag coefficient amplification due to vibration

0.631         mean square lift coefficient
0.1           2nd harmonic lift coefficient
0.15          3rd harmonic lift coefficient
0.0025        4th harmonic lift coefficient
0.025         5th harmonic lift coefficient
0.125         correlation length (1/2N or lc/L)
```

Figure 5.5: Sample input data (Constant tension cable)

```
* Summary of cable properties

tension=  349.0(lbs)
cable length=   57.3(feet)
diameter=  1.1250(inches)
added mass coeff.= 1.0
fundamenal natural freq.=  0.923(hz)
structural modal damping ratio=0.0030


* User specified sheared flow profile

location(x/L)      flow velocity(ft/sec)
  0.                      0.
  1.00                    2.15


* Total damping ratio and frequency for the mainly  excited modes

mode no.=  1   damping ratio=0.235    frequency=  0.92 Hz
mode no.=  2   damping ratio=0.131    frequency=  1.85 Hz
mode no.=  3   damping ratio=0.068    frequency=  2.77 Hz
mode no.=  4   damping ratio=0.045    frequency=  3.69 Hz


* Computational resolution

resolution in space=0.050L
resolution in frequency=0.250(hz)


* Response at location =0.125L

rms displ.=0.582(in)      rms displ./dia.=0.518
```

Figure 5.6: Input/Output data (Constant tension)

```
0.25          frequency resolution in Hz. (delf)
100           no. of frequency points, fmax = np*delf
0.05          spacial resolution
57.25         cable length in feet, L
1.125         cable outside diameter in inches
62.4          density of the surrounding fluid in Lb/ft**3
0.5764        cable weight per foot in air in Lbs./ft.
1.0           added mass coefficient
349.          constant tension in Lbs.
0.1           linearly varying component of tension (Lbs/ft)
0.17          Strouhal no.
2             Number of points specifying velocity profile
0.0,2.15      location(x/L), velocity(ft/sec) for first point
1.0,0.0       location and velocity for all succeding points
0.25          turbulence std deviation about mean velocity in ft./sec
0.003         structural modal damping ratio
1.0           drag coefficient
1.0           drag coefficient amplification due to vibration
0.631         mean square lift coefficient
0.1           2nd harmonic lift coefficient
0.15          3rd harmonic lift coefficient
0.0025        4th harmonic lift coefficient
0.025         5th harmonic lift coefficient
0.125         correlation length (1/2N or lc/L)
```

Figure 5.7: Sample input data (Linearly varying tension)

```
*  Summary of cable properties

constant tension component=  349.0 lbs
linearly varying component of tension =     0.1 lbs/ft
cable length=   57.3 ft
diameter=  1.1250 in
added mass coeff.= 1.0
fundamenal natural freq.=  0.926 Hz.
structural modal damping ratio=0.0030


* User specified sheared flow profile

location(x/L)      flow velocity(ft/sec)
  0.                      0.0
  1.00                    2.15



* Total damping ratio and frequency for the mainly  excited modes

mode no.=  1   damping ratio= 0.234     frequency=  0.93 Hz
mode no.=  2   damping ratio= 0.131     frequency=  1.85 Hz
mode no.=  3   damping ratio= 0.068     frequency=  2.78 Hz
mode no.=  4   damping ratio= 0.044     frequency=  3.71 Hz


* Computational resolution

resolution in space=0.050L
resolution in frequency=0.250(hz)


* Response at location = 0.125L

rms displ.=0.587(in)      rms displ./dia.=0.522
```

Figure 5.8: Input/Output data (Linearly varying tension)

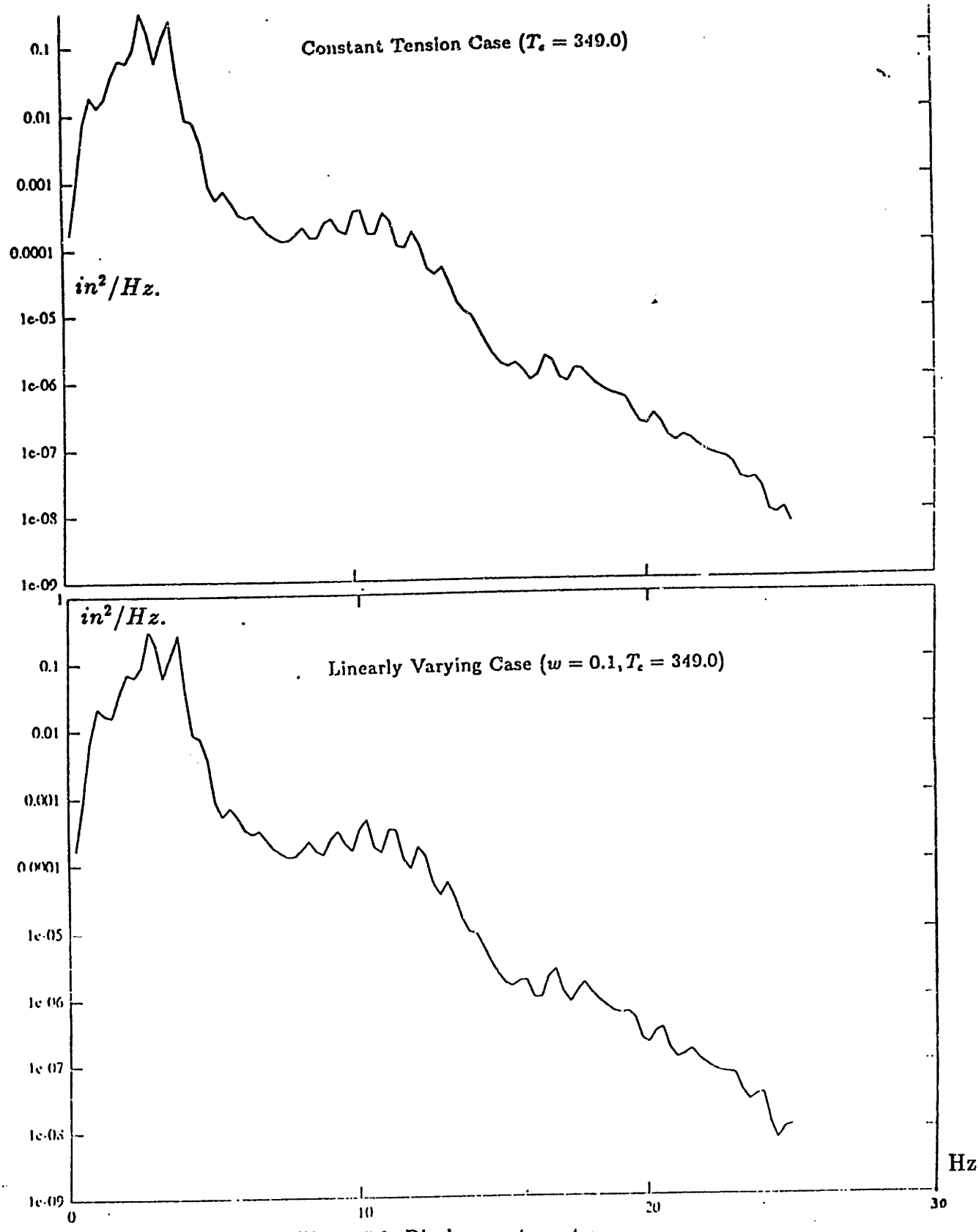

Figure 5.9: Displacement spectra

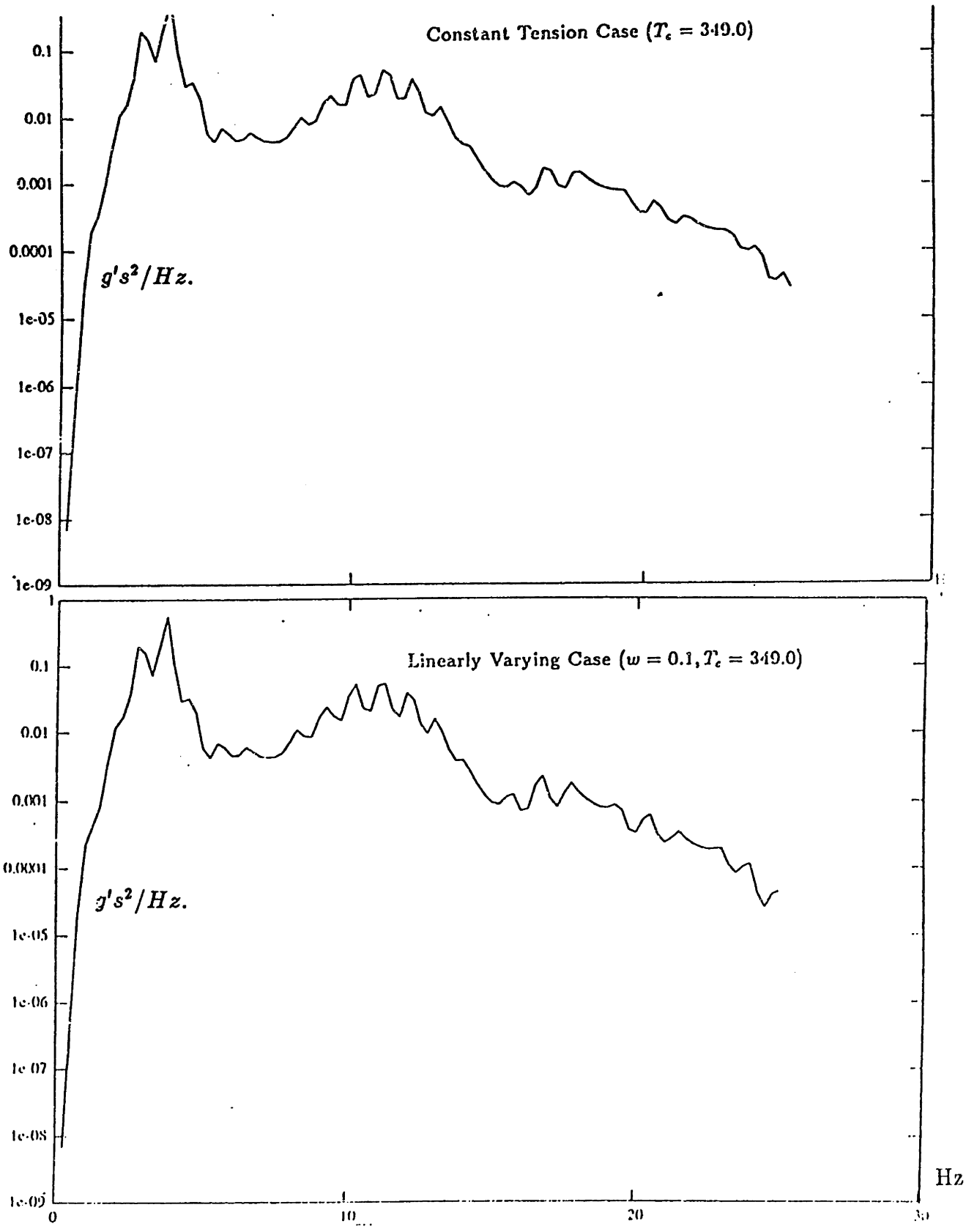

Figure 5.10: Acceleration spectra

```
0.25          frequency resolution in Hz. (delf)
100           no. of frequency points, fmax = np*delf
0.05          spacial resolution
57.25         cable length in feet, L
1.125         cable outside diameter in inches
62.4          density of the surrounding fluid in Lb/ft**3
0.5764        cable weight per foot in air in Lbs./ft.
1.0           added mass coefficient
349.          constant tension in Lbs.
5.0           linearly varying component of tension (Lbs/ft)
0.17          Strouhal no.
2             Number of points specifying velocity profile
0.0,2.15      location(x/L), velocity(ft/sec) for first point
1.0,0.0       location and velocity for all succeding points
0.25          turbulence std deviation about mean velocity in ft./sec
0.003         structural modal damping ratio
1.0           drag coefficient
1.0           drag coefficient amplification due to vibration
0.631         mean square lift coefficient
0.1           2nd harmonic lift coefficient
0.15          3rd harmonic lift coefficient
0.0025        4th harmonic lift coefficient
0.025         5th harmonic lift coefficient
0.125         correlation length (1/2N or lc/L)
```

Figure 5.11: Sample input data (Linearly varying tension)

```
* summary of cable properties

constant tension component=  349.0(lbs)
linearly varying coefficient of tension =     5.0
cable length=   57.3(feet)
diameter=  1.1250(inches)
added mass coeff.= 1.0
fundamenal natural freq.=  1.084(hz)
structural modal damping ratio=0.0030


* user specified sheared flow profile

location(x/L)      flow velocity(ft/sec)
  0.                    0.0
  1.00                  2.15



* Total damping ratio and frequency for the mainly  excited modes

mode no.=  1   damping ratio= 0.183    frequency=  1.08 Hz
mode no.=  2   damping ratio= 0.105    frequency=  2.17 Hz
mode no.=  3   damping ratio= 0.040    frequency=  3.25 Hz
mode no.=  4   damping ratio= 0.060    frequency=  4.33 Hz


* Computational resolution

resolution in space=0.050L
resolution in frequency=0.250(hz)


* Response at location =0.125L

rms displ.=0.672(in)      rms displ./dia.=0.598
```

Figure 5.12: Input/Output data (Linearly varying tension)

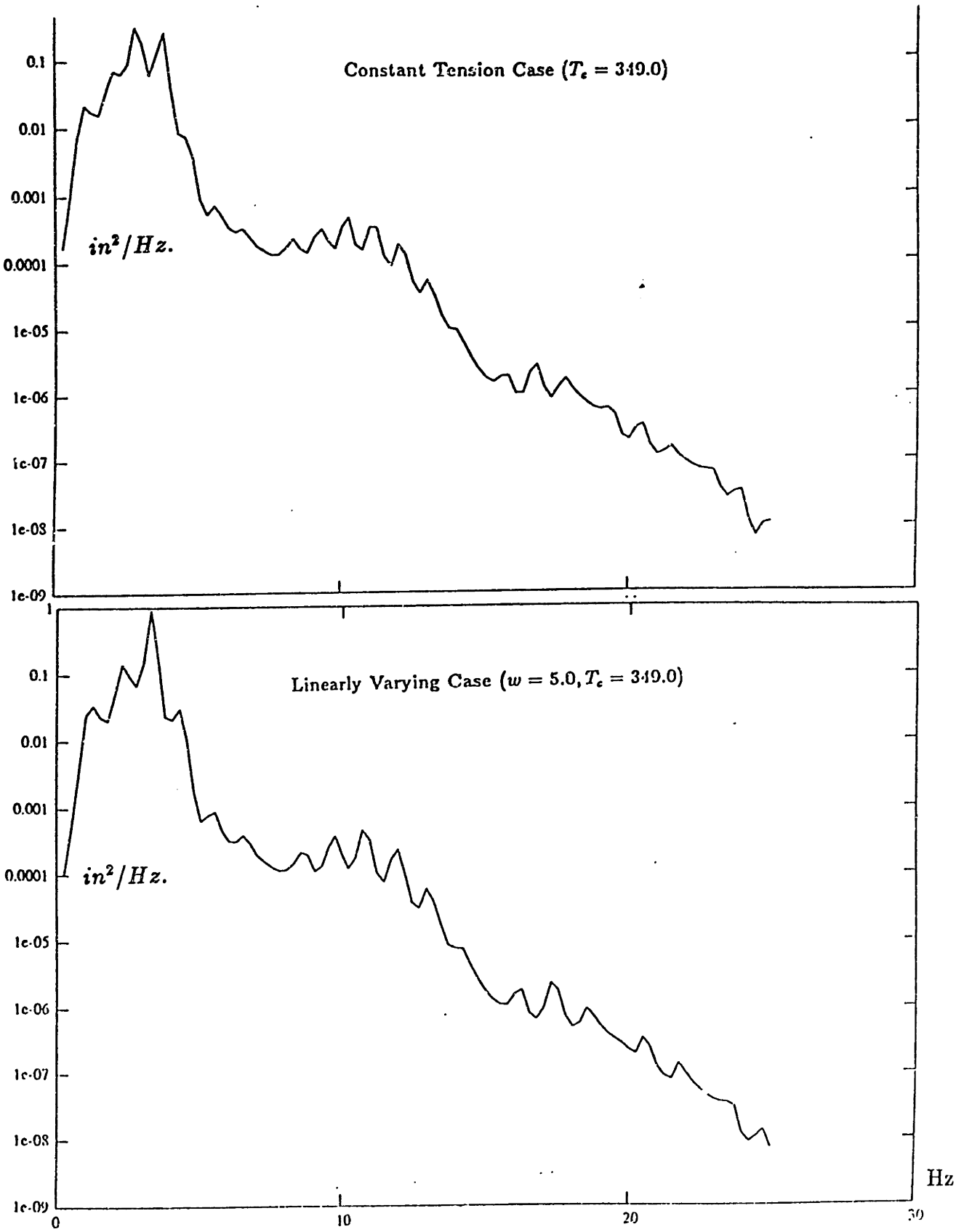

Figure 5.13: Displacement spectra

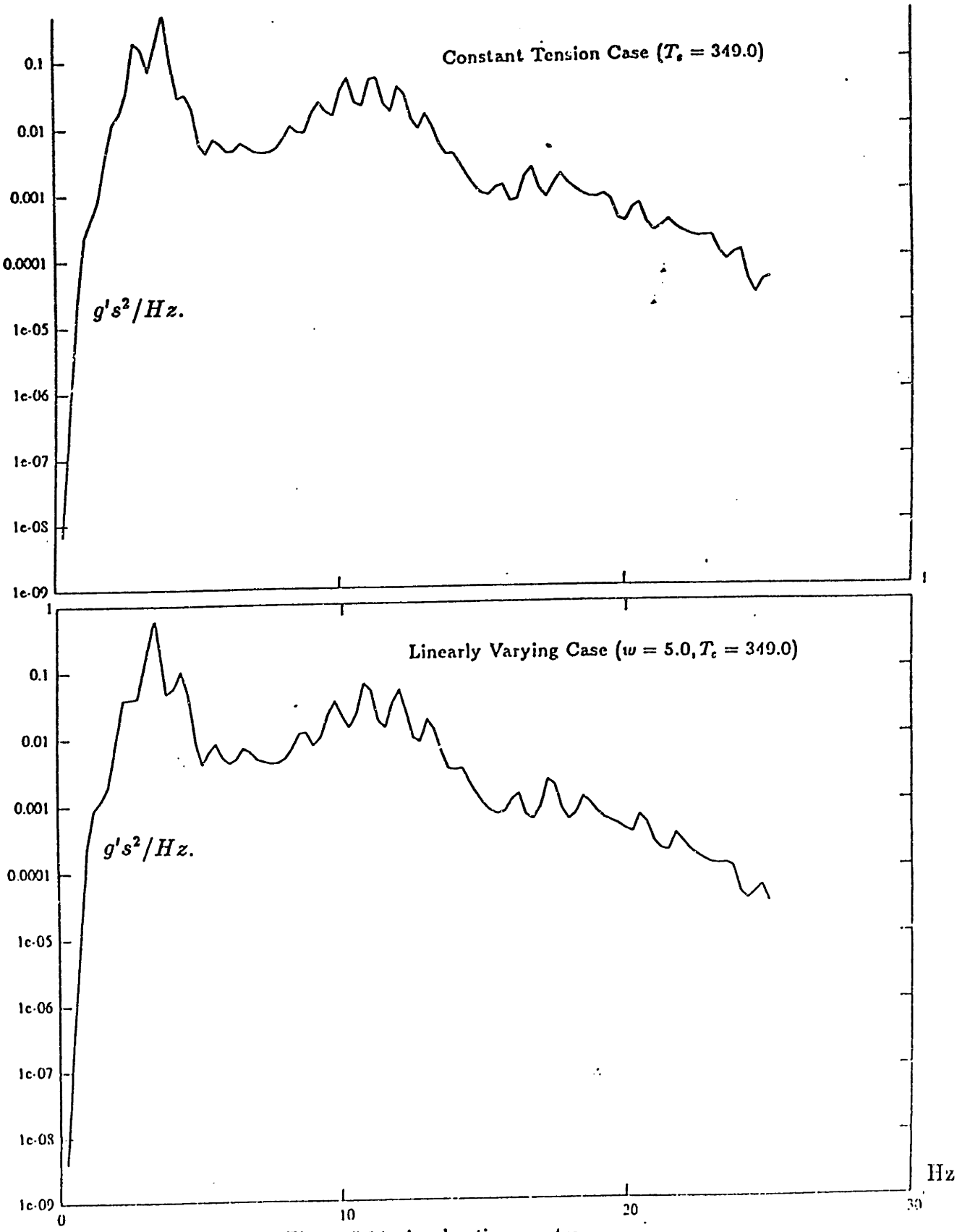

Figure 5.14: Acceleration spectra

foot, ($\underline{a} = 0.57$), necessitating the use of the linearly varying tension model.

The shear current profile for this case varied linearly from s/L = 1.0 to s/L = 0.75 with corresponding velocities in feet/sec of 4.0 and 3.8. The current profile for the remainder of the cable decays exponentially from 3.8 feet/sec at s/L = 0.75 to 0.0 feet/sec at s/L = 0.0. The value of T_c for this case was 100,000 pounds. Figure 5.15 is the corresponding computer input file which includes all necessary input parameters. Given the tension variation of 28.6 pounds per foot this resulted in a tension of 100,000 pounds at the cable anchor and 156,000 pounds at the surface. These properties resulted in a natural frequency for the cable of 0.05 hertz, and the corresponding Strouhal frequencies resulted in the mainly excited modes being 1 - 16. Damping ratios for these modes varied from 72 percent for the first mode to about 3 percent for the sixteenth mode. For a more detailed listing of output information see figure 5.16 which includes the more important program output information

Once again dominant response is seen in the frequency range corresponding to that of the mainly excited modes. But also, one can see that significant contributions come from non-resonant modes. The standard convention for this model is that the spectrum bandwidth must include 5 times the highest Strouhal frequency. For this case the highest Strouhal frequency is 0.84 Hz., therefore the bandwidth must include $(0.84)(5) = 4.2Hz$. From the corresponding displacement and acceleration spectra (figure 5.17) one can see that the significant response occurs in the 0 - 4 Hz. range.

The resulting rms displacement value for the location $s = 0.875L$ from figure 5.16 is seen to be 5.929 inches. This response location is at a point on the cable where the flow velocity is relatively large. If one were to choose a response location where the profile is lower, say at $s = 0.125L$, then we would expect a lower response value. This case was tested and the resulting rms displacement value was found to be 1.950 inches. From this one can see the significant effect a sheared velocity profile has on system response.

The large cable also presents a new problem, that is, what effect if any does

structural rigidity (EI) have on the response of the system. We examine this effect by incorporating the tension and effective stiffness into the characteristic equation for natural frequency. This is done by taking the simple constant tension cable equation and using the average tension value from our case and the corresponding values for E and I.

The equation takes the form;

$$\omega_n = \frac{\pi^2}{L^2}\left(\frac{EI}{\rho A}\right)^{1/2}\left(n^4 + \frac{n^2 TL}{\pi^2 EI}\right)^{1/2} \tag{5.19}$$

$$= \left(\frac{n^2\pi^2}{L^2\rho A}\right)^{1/2}\left(\frac{n^2\pi^2 EI}{L^2} + T\right)^{1/2} \tag{5.20}$$

$$= \frac{n\pi}{L}\sqrt{\frac{T}{\rho A}}\left(\frac{n^2\pi^2 EI}{L^2 T} + 1\right)^{1/2} \tag{5.21}$$

The leading term in equation 5.20 is seen to be the expression for the fundamental natural frequencies for a string under constant tension. The term in parenthesis represents what effect the stiffness terms have on natural frequency. If we choose the corresponding parameters for sixteenth mode oscillation we see that including the effects of stiffness resulted in an 8 percent change in natural frequency from the case of the simple string. From this one can conclude that the effects of structural rigidity (EI) on the response of the system are negligible and for our purposes can be neglected.

```
2000 Foot Cable (Tension Variation = 28.6 Lbs/ft.)

0.01          frequency resolution in Hz. (delf)
500           no. of frequency points ,fmax=np*delf
0.01          spacial resolution (delx/L)
2000          cable length in feet ,L
9.625         cable outer diameter in inches
62.4          density of the surrounding fluid in lb/ft**3
60.14         cable weight per foot in air in pounds/foot
1.0           added mass coefficient
1.0e05        lumped constant tension in pounds
28.6          coefficient of linearly varying tension (lb/ft)
0.17          Strouhal no.
7             number of points specifying velocity profile
1.0 ,4.0      location(x/L), velocity(ft/sec) for first point
0.75,3.8      location and velocity of each succeeding point
0.625,2.7
0.5,1.85
0.375,1.2
0.25,0.5
0.0,0.0
0.25          turbulence std deviation about mean velocity in ft/sec
0.003         structural modal damping
1.0           drag coefficient
1.0           drag coefficient amplification due to vibration
0.631         mean square lift coefficient
0.1           2nd harmonic lift coef.
0.15          3rd harmonic lift coef.
0.0025        4th harmonic lift coef.
0.025         5th harmonic lift coef.
0.020         correlation length (1/2N or lc/L)
```

Figure 5.15: Input data (Linearly varying tension)

```
* Summary of cable properties

constant tension component=100,000(lbs)
linearly varying coefficient of tension =   28.6
cable length= 2000.0(feet)
diameter=  9.6250(inches)
added mass coeff.= 1.0
fundamenal natural freq.=  0.053(hz)
structural modal damping ratio=0.0030


* User specified sheared flow profile

location(x/L)      flow velocity(ft/sec)
  1.00                    4.00
  0.75                    3.80
  0.63                    2.70
  0.50                    1.85
  0.38                    1.20
  0.25                    0.50
  0.                      0.

* Total damping ratio and frequency for the mainly  excited modes

mode no.=  1   damping ratio= 0.797    frequency=  0.05 Hz
mode no.=  2   damping ratio= 0.411    frequency=  0.11 Hz
mode no.=  3   damping ratio= 0.275    frequency=  0.16 Hz
mode no.=  4   damping ratio= 0.208    frequency=  0.21 Hz
mode no.=  5   damping ratio= 0.167    frequency=  0.26 Hz
mode no.=  6   damping ratio= 0.140    frequency=  0.32 Hz
mode no.=  7   damping ratio= 0.121    frequency=  0.37 Hz
mode no.=  8   damping ratio= 0.105    frequency=  0.42 Hz
mode no.=  9   damping ratio= 0.093    frequency=  0.48 Hz
mode no.= 10   damping ratio= 0.085    frequency=  0.53 Hz
mode no.= 11   damping ratio= 0.077    frequency=  0.58 Hz
mode no.= 12   damping ratio= 0.070    frequency=  0.63 Hz
mode no.= 13   damping ratio= 0.049    frequency=  0.69 Hz
mode no.= 14   damping ratio= 0.038    frequency=  0.74 Hz
mode no.= 15   damping ratio= 0.049    frequency=  0.79 Hz
mode no.= 16   damping ratio= 0.053    frequency=  0.84 Hz


* Computational resolution

resolution in space=0.010L
resolution in frequency=0.010(hz)


* Response at location =0.875L

rms displ.=5.929(in)      rms displ./dia.=0.616
```

Figure 5.16: Input/Output data (Linearly varying tension)

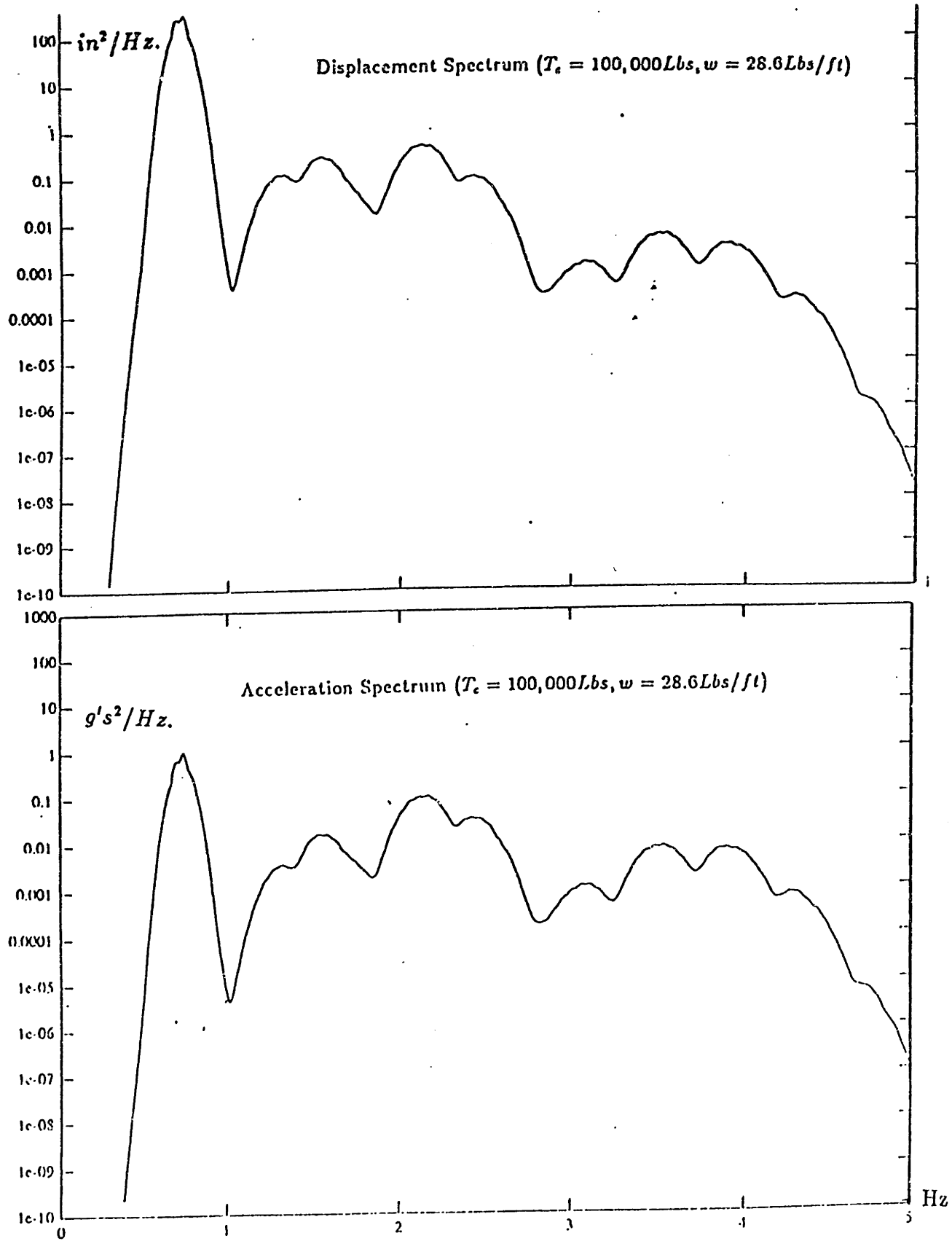

Figure 5.17: Response spectra

Chapter 6

Summary

This paper set out to develop an accurate response prediction model for a non-constant tension cable. Examples were done in which the response prediction model was tested for the specific case of linear tension variation. Although this particular case was chosen , the damping and response prediction models are also valid for more complex tension variation (quadratic, exponential).

It was seen that for the case of spatially varying tension it was necessary to derive more complex relations for the system natural frequencies and mode shapes based on the corresponding non-constant tension governing equations. From these relations it was possible to determine the modal damping ratios and constants for the excited modes. The system damping was seen to be a major factor in the system response, therefore an accurate model taking into account spatially varying tension effects was needed.

To accurately predict these damping values it was necessary to take into account the effects the vortex shedding process had on the response. The parameter H was defined which effectively partitioned the cable into a power-in region where the vortex shedding and cylinder motion are correlated, and a power-out region where the cable is damped. H was seen to be dependent on the correlation length which is the separation distance between two locations which causes the excitation to drop below a specified value.

In testing the response prediction model it was seen that for sufficiently small

values of tension variation coefficient ($a < 0.2$) the linearly varying tension cable can be effectively modelled as a constant tension case. The examples tested show that for both Greens function and response spectra values, the slowly varying tension cable and constant tension cable were equivalent for values of tension variation coefficient, a, less than 0.2. For values of a above this it was seen that the constant tension model no longer accurately predicted response values and that the more complicated spatially varying model needed to be used.

Finally it was seen how the model responded when applied to a more practical situation of a deep water marine cable. For the given cable, the tension variation coefficient was calculated and it was found that it was necessary to use the linearly varying tension model. For this cable configuration and current profile a significantly greater number of modes were excited as compared to the cable examined previously. The response spectra were calculated and corresponding rms response found for several specified locations and it was seen that the sheared velocity profile had a significant effect on the cable response values for different locations in the flow.

The model has been seen to be effective in calculating response values for cables excited in their lower modes. Work is now being conducted to attempt to expand the model such that it can effectively predict the response of cables which behave as if they were infinite in length.

Bibliography

[1] T.Y. Chung. *Vortex Induced Vibration of Flexible Cylinders in Sheared Flows.* PhD thesis, Massachusetts Institute of Technology, 1987.

[2] M.S. Triantafyllou. Preliminary design of mooring systems. *Journal of Ship Research*, 26(1), March 1983.

[3] J.K. Vandiver and T.Y. Chung. *Hydrodynamic Damping on Flexible Cylinders in Sheared Flow.* Offshore Technology Conference, OTC 5524, April, 1987.

[4] M.S. Triantafyllou and J.M. Burgess. *Mooring Dynamics for Offshore Applications.* Technical Report, MIT Sea Grant Program, 1986.

[5] R.D. Blevins. Flow Induced Vibration. Van Nostrandt Reinhold Co., 1977.

[6] F.B. Hildebrand. Advanced Calculus for Applications. Prentice Hall Inc., 1976.

[7] H.M. Irvine. Cable Structures. MIT Press, 1981.

[8] A.M. Nayfeh. Perturbation Methods. John Wiley and Sons, 1973.

[9] J.N. Newman. Marine Hydrodynamics. MIT Press, 1977.

Appendix A

Green's Function Expansion

Given the general form of the Green function;

$$G(s,x) = \frac{\sinh \int_0^s \frac{i\mu ds}{\sqrt{T(s)/m}} \sinh \int_x^L \frac{i\mu ds}{\sqrt{T(s)/m}}}{i\mu \sqrt[4]{T(s)T(x)} \sinh \int_0^L \frac{i\mu ds}{\sqrt{T(s)/m}}}, 0 \leq s \leq x \tag{A.1}$$

$$G(s,x) = \frac{\sinh \int_s^L \frac{i\mu ds}{\sqrt{T(s)/m}} \sinh \int_0^x \frac{i\mu ds}{\sqrt{T(s)/m}}}{i\mu \sqrt{m} \sqrt[4]{T(s)T(x)} \sinh \int_0^L \frac{i\mu ds}{\sqrt{T(s)/m}}}, x \leq s \leq L \tag{A.2}$$

it is possible to perform the following complex expansion:

$$\sinh \int_0^L \frac{i\mu ds}{\sqrt{T(s)/m_t}} = \sinh[i\mu {m_t}^{1/2} \frac{2}{w}[(T_c + w \cdot L)^{1/2} - (T_c)^{1/2}]] \tag{A.3}$$

Where we define $A = \mu {m_t}^{1/2} \frac{2}{w}[(T_c + w \cdot L)^{1/2} - (T_c)^{1/2}]$

$$\sinh \int_0^s \frac{i\mu ds}{\sqrt{T(s)/m}} = \sinh[i\mu {m_t}^{1/2} \frac{2}{w}[(T_c + w \cdot s)^{1/2} - (T_c)^{1/2}] \tag{A.4}$$

$B = \mu {m_t}^{1/2} \frac{2}{w}[(T_c + w \cdot s)^{1/2} - (T_c)^{1/2}]$

$$\sinh \int_x^L \frac{i\mu ds}{\sqrt{T(s)/m_t}} = \sinh[i\mu {m_t}^{1/2} \frac{2}{w}[(T_c + w \cdot L)^{1/2} - (T_c + w \cdot x)^{1/2}] \tag{A.5}$$

$C = \mu {m_t}^{1/2} \frac{2}{w}[(T_c + w \cdot L)^{1/2} - (T_c + w \cdot x)^{1/2}]$

$$\sinh \int_s^L \frac{i\mu ds}{\sqrt{T(s)/m_t}} = i\mu \sqrt{m_t} \frac{2}{w}[(T_c + w \cdot L)^{1/2} - (T_c + w \cdot s)^{1/2}] \tag{A.6}$$

$$D = \mu\sqrt{m_t}\frac{2}{w}[(T_c + w{\cdot}L)^{1/2} - (T_c + w{\cdot}s)^{1/2}]$$

$$\sinh\int_0^x \frac{i\mu ds}{\sqrt{t(s)/m_t}} = i\mu\sqrt{m_t}\frac{2}{w}[(T_c + w{\cdot}x)^{1/2} - (T_o)^{1/2}] \tag{A.7}$$

$$E = \mu\sqrt{m_t}\frac{2}{w}[(T_c + w{\cdot}x)^{1/2} - (T_c)^{1/2}]$$

Then;

$$G(s,x) = \frac{\sinh iB \sinh iC}{i\mu m_t^{1/2}\sqrt[4]{T(s)T(x)}\sinh iA} 0{\le}s{\le}x \tag{A.8}$$

$$G(s,x) = \frac{\sinh iD \sinh iE}{i\mu\sqrt{m_t}\sqrt{T(s)T(x)}\sinh iA} x{\le}s{\le}L \tag{A.9}$$

$\sinh iA = \frac{e^{iA}-e^{-iA}}{2}$

$\sinh iB = \frac{e^{iB}-e^{-iB}}{2}$

$\sinh iC = \frac{e^{iC}-e^{-iC}}{2}$

$\sinh iD = \frac{e^{iD}-e^{-iD}}{2}$

$\sinh iE = \frac{e^{iE}-e^{-iE}}{2}$, and then

$$G(s,x) = \frac{(\frac{e^{iB}-e^{-iB}}{2i})(\frac{e^{iC}-e^{-iC}}{2i})}{\frac{(e^{iA}-e^{-iA})}{2i}}\frac{1}{\mu\sqrt{m_t}\sqrt[4]{T(s)T(x)}} \tag{A.10}$$

$$= \frac{\sin B \sin C}{\sin A}\frac{1}{\mu\sqrt{m_t}\sqrt[4]{T(s)T(x)}} 0{\le}s{\le}x \tag{A.11}$$

$$G(s,x) = \frac{(\frac{e^{iD}-e^{-iD}}{2i})(\frac{e^{iE}-e^{-iE}}{2i})}{(\frac{e^{iA}-e^{-iA}}{2i})}\frac{1}{\mu\sqrt{m_t}\sqrt[4]{T(s)T(x)}} \tag{A.12}$$

$$= \frac{\sin D \sin E}{\sin A}\frac{1}{\sqrt[4]{T(s)T(x)}\mu\sqrt{m_t}} \tag{A.13}$$

Next, we expand the complex frequency, μ. We have already stated that,

$A = \mu\sqrt{m_t}\frac{2}{w}[(T_c + w \cdot L)^{1/2} - (T_c)^{1/2}]$

$= \mu \cdot aa$

$\mu = \omega^2 + i\frac{b}{m_t}$, and let $mur = \omega^2$, and $mui = \frac{b}{m}$.

Next, we expand the term aa into its real and imaginary components;

$p1 = aa \cdot mur$

$q1 = aa \cdot mui$

Which results in,

$\sin A = \sin p1 \cosh q1 + i \cos p1 \sinh q1$

The same is then done for terms B, C, D and E such that;

$B = \mu \cdot bb$

$p2 = bb \cdot mur$

$q2 = bb \cdot mui$

$\sin B = \sin p2 \cosh q2 + i \cos p2 \sinh q2$,and

$C = \mu \cdot cc$

$p3 = cc \cdot mur$

$q3 = cc \cdot mui$

$\sin C = \sin p3 \cosh q3 + i \cos p3 \sinh q3$

$D = \mu \cdot dd$

$p4 = dd \cdot mur$

$q4 = dd \cdot mui$

$\sin D = \sin p4 \cosh q4 + i \cos p4 \sinh q4$

$E = \mu \cdot ee$

$p5 = ee \cdot mur$

$q5 = ee \cdot mui$

$\sin E = \sin p5 \cosh q5 + i \cos p5 \sinh q5$

Performing the necessary complex expansions on these terms results in the usable forms of the Green's function as;

$$GRR(s,x) = \frac{mur(nr1 + nr2) + mui(ni1 - ni2)}{dr1\sqrt{m_t}\sqrt[4]{T(s)T(x)}(mur^2 + mui^2)} \tag{A.14}$$

$$GRI(s,x) = \frac{mur(ni1 - ni2) - mui(nr1 + nr2)}{dr1\sqrt{m_t}\sqrt[4]{T(s)T(x)}(mur^2 + mui^2)} \tag{A.15}$$

$$GRR(s,x) = \frac{mui(nr3 + nr4) + mui(ni3 - ni4)}{dr2\sqrt{m_t}\sqrt[4]{T(s)T(x)}(mur^2 + mui^2)} \tag{A.16}$$

$$GRI(s,x) = \frac{mur(ni3 - ni4) - mui(nr3 + nr4)}{dr2\sqrt{m_t}\sqrt[4]{T(s)T(x)}(mur^2 + mui^2)} \tag{A.17}$$

where;

$$nr1 = \sin p1 \cosh q1[\sin p2 \cosh q2 \sin p3 \cosh q3 - \cos p2 \sinh q2 \cos p3 \sinh q3]$$

$$nr2 = \cos p1 \sinh q1[\cos p2 \sinh q2 \sin p3 \cosh q3 + \cos p3 \sinh q3 \sin p2 \cosh q2]$$

$$nr3 = \sin p1 \cosh q1[\sin p4 \cosh q4 \sin p5 \cosh q5 - \cos p4 \sinh q4 \cos p5 \sinh q5$$

$$nr4 = \cos p1 \sinh q1[\cos p4 \sinh q4 \sin p5 \cosh q5 + \cos p5 \sinh q5 \sin p4 \cosh q4$$

$$ni1 = \sin p1 \cosh q1[\cos p2 \sinh q2 \sin p3 \cosh q3 + \cos p3 \sinh q3 \sin p2 \cosh q2]$$

$$ni2 = \cos p1 \sinh q1[\sin p2 \cosh q2 \sin p3 \cosh q3 - \cos p2 \sinh q2 \cos p3 \sinh q3$$

$$ni3 = \sin p1 \cosh q1[\cos p4 \sinh q4 \sin p5 \cosh q5 + \cos p5 \sinh q5 \sin p4 \cosh q4$$

$$ni4 = \cos p1 \sinh q1[\sin p4 \cosh q4 \sin p5] \cosh q5 - \cos p4 \sinh q4 \cos p5 \sinh q5$$

$$dr1 = \sin p1^2 \cosh q1^2 + \cos p1^2 \sinh q1^2$$

$$dr1 = dr2$$